CALIFORNIA PATH PROGRAM
INSTITUTE OF TRANSPORTATION STUDIES
UNIVERSITY OF CALIFORNIA, BERKELEY

An Empirical and Theoretical Study of Freeway Weave Bottlenecks

Joon ho Lee, Michael J. Cassidy

California PATH Research Report
UCB-ITS-PRR-2009-13

This work was performed as part of the California PATH Program of the University of California, in cooperation with the State of California Business, Transportation, and Housing Agency, Department of Transportation, and the United States Department of Transportation, Federal Highway Administration.

Final Report for Task Order 6304

February 2009

ISSN 1055-1425

MOU/TO 6304:

Part I: An Empirical and Theoretical Study

of

Freeway Weave Bottlenecks

by

Joon ho Lee

and

Professor Michael J. Cassidy

ACKNOWLEDGMENTS

The research team is especially grateful to those Caltrans personnel who offered guidance as members of the Advisory Committee. Those members were Sam Toh, Scott Eades, St eve Hague, Zhongren Wang, Rodney Oto, Jose Mujica, Vu H. Nguyen, Fred Yazden and Tam Nguyen.

ABSTRACT

The present research performed an empirical and theoretical analysis on what triggers bottleneck activations and discharge flow changes in weaving sections. Investigations revealed that changes in the spatial distributions of mandatory lane changes, especially for Freeway-to-Ramp (F-R) maneuvers, led to variations in bottleneck discharge flows. When the F-R maneuvers were concentrated near on-ramp, they became more disruptive, resulting in bottleneck activations with reductions in discharge flows. Findings further indicate that the spatial distributions of these lane changes, in turn, were dictated by the traffic conditions in the auxiliary lane. On-ramp flow reductions increased the attractiveness of the auxiliary lanes, thus motivating F-R drivers to perform their maneuvers nearer the on-ramp, and vice versa. A micro-simulation model was developed based on the observed lane-changing behaviors, and it successfully reproduced the observed mechanisms of weaving bottleneck flows.

Keywords: Weaving, Weaving sections, Simulation, Discrete choice modeling

EXECUTIVE SUMMARY

Though there have been numerous studies of freeway weaving sections (i.e., segments in which an on-ramp is followed by an off-ramp), there remains a significant lack of empirical and theoretical understanding of the traffic behavior that causes weaving sections to become bottlenecks with varying discharge flows. The present research entails empirical analysis and theoretical modeling of what triggered the bottleneck activations and discharge flow changes in two freeway weaving sections. Both sites were recurrent bottlenecks during the rush, and investigations revealed that changes in the spatial patterns of vehicular lane-changes, especially among Freeway-to-Ramp (F-R) maneuvers, caused variations in bottleneck discharge flow. When the F-R maneuvers were concentrated near a weaving section's on-ramp, they became more disruptive, resulting in bottleneck activations with diminished discharge flows. Findings further indicated that the spatial distributions of these lane changes, in turn, were dictated by the traffic conditions in the auxiliary lane (i.e., the lane connecting the off-ramp to the upstream on-ramp). Reductions in on-ramp flows increased the attractiveness of the auxiliary lane, thus motivating F-R drivers to perform their maneuvers nearer the on-ramp. Conversely, increases in on-ramp flows motivated F-R drivers to perform their maneuvers over a wider stretch of the weaving section.

Based on these empirical findings, the study formulated a theory for *mandatory* lane changing (i.e., lane changes required of a desired Origin-Destination pattern); and used this theory to enhance an existing microsimulation model of car-following and lane

changing. With this new theory, the driver's decision to attempt a lane change is determined by the vehicle's distance from the downstream end of the weaving section's diverge area, the number of lanes to be crossed in reaching the desired destination, and the difference in densities between the driver's target lane and her current one. The model reproduces the observed mechanisms of bottleneck activation and discharge flow changes in weaving sections. These empirical findings, together with the outcomes of simulation, point to two key features of driver behavior in weaving sections: i) traffic conditions (especially densities) in an auxiliary lane influence drivers' decisions regarding where to perform mandatory lane changes; and ii) the spatial distributions of lane changes determine weave bottleneck discharge flows.

The model was developed into an executable standalone program in MATLAB so that it can help users, especially Caltrans employees, to analyze the traffic characteristics of weaving bottlenecks and design weaving sections. The inputs of the program include traffic demands by vehicles' Origin-Destination and geometric configurations (e.g., length of the weaving section of interest, number of lanes, free-flow speed, and etcetera) The program generates simulation results including total delays as well as delay for each OD maneuver. Further, it plots oblique cumulative vehicle count curves that display discharge flows and average speeds. The simulation program is based on the empirical findings of the present study, and therefore it is only applicable to weaving sections with connected (full) auxiliary lanes. Applications of the program to acceleration or deceleration auxiliary lanes are not recommended.

TABLE OF CONTENTS

FIGURES

TABLES

CHAPTER 1. INTRODUCTION

Freeway weaving sections form where an on-ramp is followed closely by an off-ramp, such that vehicles' merging and diverging maneuvers co-exist; see, for example, figure 1. There are two types of vehicle's lane-changing maneuvers in weaving sections: (i) mandatory lane changes needed to achieve a particular O-D movement; and (ii) optional lane changes that drivers might perform to improve their travel speeds. Vehicular conflicts that arise due to these lane-changing maneuvers, particularly between weaving (F-R & R-F; see figure 1) and non-weaving (F-F & R-R) traffic streams, can cause weaving areas to become active bottlenecks and their discharge flows to diminish. The discharge flows from a weaving bottleneck are defined here as the sum of the freeway and off-ramp outflows.

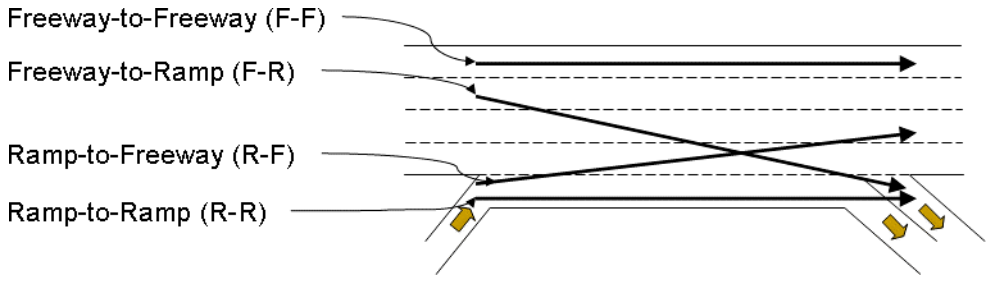

Figure 1. Origin-Destination (O-D) maneuvers in a weaving section

1.1. Problem Overview

Research on freeway weaving section design and analysis has a long history. It is one that is characterized by a near-constant stream of proposed models, most of which attempt to predict vehicle travel speeds within weaving sections. However, using vehicle

speeds as a weaving section's performance metric has a number of limitations (e.g., speeds are unreliable for assessing capacity and cannot be used to assess the system-wide delays that arises upstream of weaving sections). In light of these drawbacks, there have been several more recent attempts to estimate weaving section capacity. However, most of these studies did not verify that their measurements were from active weaving bottlenecks (and therefore could not verify that their measured flows were bottlenecks' capacity); and did not examine the mechanisms (i.e., lane changes) that affect weaving section capacity. The present research explores freeway weaving from a microscopic perspective in an attempt to understand and model the mechanisms that trigger weave bottlenecks, and that dictate changes in their discharge flows.

1.2. Research Objectives

The objectives of this research are (i) to empirically study the traffic details that cause freeway weaving sections to become active bottlenecks and that trigger changes in discharge flows; and (ii) to advance existing theories to capture these details, and to test the advancements with real data.

1.3. Report Outline

Chapter 2 of this report summarizes previous efforts to develop mathematical tools for analyzing freeway weaving sections and/or to develop weaving models. Chapter 3 describes the two freeway weaving sites used for the present study and the empirical findings from these sites. Chapter 4 describes a theoretical model formulated to

reproduce empirical findings at both study sites; and the tests of this theory against real data. Finally, Chapter 5 presents a summary, future research plans, and concluding remarks.

CHAPTER 2. LITERATURE REVIEW

Numerous studies have been conducted on freeway weaving sections, and most of these have been efforts to improve procedures in the Highway Capacity Manual. Many of these have produced models for predicting vehicle travel speeds within weaving sections. Curiously, a good many studies claimed to have developed models of weaving capacity, yet there seem to be only two studies to have examined weaving sections that were active bottlenecks. In spite of these efforts, the models were typically found to be inconsistent and unreliable, and thus the literature traces a long series of attempts to develop improved models.

Section 2.1 describes and critiques the speed-prediction models that have shaped much of the current thinking on weaving analyses. Models of weaving area capacity are briefly discussed in section 2.2. Section 2.3 summarizes previous empirical efforts to understand traffic in weaving sections that actually were bottlenecks. Section 2.4 describes the models of driver lane-changing behavior that will be adapted for the present work.

2.1. Speed Prediction Models

Descriptions of speed prediction models are given below. This is followed with a critique.

A methodology for weaving design and analysis was first presented in the 1950 Highway Capacity Manual (HCM). It predicted flows and speeds within freeway weaving sections, and the results were illustrated in a graphic form. The model was based on field observations at six sites near Washington D.C. The researchers reported (seemingly as an aside) that reductions in speed and discharge flows occurred whenever traffic density (the number of vehicles per distance) in the weaving section exceeded a critical value.

An update to the above procedure was furnished in a nomographic form in the next version of the HCM (1965). In the newer version, speeds depend on the length and width of the weaving section. The 1965 HCM also reported that a weaving section became congested when the sum of F-R and R-F flows exceeded the capacity of the two rightmost lanes, but this insight was not captured by the model

In 1975, Pignataro, et al. (1975) developed the PINY (Polytechnic Institute of New York) method. It involved the use of a nomograph to separately predict speeds of weaving and of non-weaving vehicles for a given number of lanes, weaving section length, volumes of weaving and of non-weaving vehicles.

In 1979, Leisch proposed an extension of the nomograph procedure of the 1965 HCM. Like the PINY method, the Leisch extension predicted speeds of weaving vehicles as a function of the weaving section length, the number of lanes, and weaving volume. However, unlike PINY method, the Leisch procedure did not estimate the speeds of non-weaving vehicles.

Users reportedly found nomograph procedures difficult to apply, and the two weaving procedures (PINY and Leisch) often yielded very different predictions. Thus, a modified procedure was developed by JHK and Associates. This model consists of regression-based equations used to predict the average travel speeds of weaving and of non-weaving vehicles. The 1985 HCM included a revised version of this JHK method.

Fazio and Rouphail (1986) examined three of the above-cited weaving procedures (Leisch, JHK, and 1985 HCM), and proposed a new speed-prediction regression-based technique (Fazio Method). Inputs to the model include the weaving area's geometry and the total number of lane-changing maneuvers required by F-R and by R-F drivers operating within the section.

Cassidy, et al. (1989) enhanced an existing microscopic computer model (INTRAS[1]) and calibrated its parameters using video data from eight weaving sections in California. The researchers tested this model, along with six existing methods (1965 HCM, Leisch, PINY, JHK, 1985 HCM, and Fazio) against real data. They found that the average speeds predicted by INTRAS were closer to the field data than those predicted by the analytical methods, concluding that microsimulation is a useful tool for analyzing weaving segments. They also found that:

- congestion at freeway weaving sections was often triggered by queue formation in a single lane:

[1] Fazio, J., Rouphail, N. (1990)

- vehicle speeds were insensitive to weaving section geometry over the range of values in the data set; and thus
- average vehicle travel speed may not be an ideal measure of effectiveness for weaving sections.

Further research in Cassidy and May (1991) confirmed that the operation of weaving sections is influenced largely by what occurs in individual lanes. The researchers proposed an analytical procedure for estimating capacity and speed in weaving sections. The procedure predicts how F-R and R-F vehicles are distributed at any locations along the two rightmost lanes (the auxiliary lane and its adjacent lane). These estimates generate estimation of total outflows. The researchers tested this analytical procedure with extensive simulation modeling using INTRAS.

Additional empirical study by Cassidy, et al. (1993) revealed some important considerations:

- the F-R and R-F movements creates very high flows at points near the on-ramp within the auxiliary lane,
- the highest proportion of lane-changing activity occurs near these points as well.

Finally, the 2000 HCM estimated the speed of weaving and of non-weaving streams, using the method of the earlier edition (1985 HCM). It also included a series of new

tables that provide capacity estimates for various weaving section geometries.

Even setting aside the insensitivity of speeds to flows (as noted in Cassidy, et al. (1989)), the time spent traveling in a weaving section (even at low speeds) can be trivial when compared with the large delays that may occur if the weaving section becomes a bottleneck and generates a queue that grows long upstream. Thus the primary objective in weaving analysis should be to determine whether a weaving section becomes a bottleneck; and the bottleneck's capacity (maximum queue discharge flows) should be the metric of interest.

2.2. Capacity Prediction Models

In light of the above, there have been several more recent attempts to estimate the capacity of freeway weaving sections.[2] Some of these tested microsimulation models such as INTRAS, FORSIM, and INTEGRATION (e.g., Stewart et al. 1996; Vermijis 1998; Rakha and Zhang 2004). Others focused on gap-acceptance with linear optimization models (e.g., Lertworawanich and Elefteriadou 2002, 2003, 2004), or regression models (e.g., Cassidy et al. 1989; Kwon et al. 1999, 2000; HCM 2000). These efforts led to the recommendations concerning the use of existing models, or to modifications of these models, to estimate weaving section capacity.

---

[2] The capacity of a weaving segment is claimed by some to be any combination of flows that causes the density to reach the LOS E/F boundary condition of 43 pc/mi/ln (passenger car per mile per lane) for freeways or 40 pc/mi/ln for multilane highways. (2000 HCM)

Researchers sought to estimate parameters in their models using real traffic data. They did not, however, verify that their empirical measurements were from active bottlenecks[3]. As such, the outflows measured in these studies may not have actually reflected weaving area capacity. Moreover, there were no attempts to use real data to explore the traffic details that trigger bottleneck activation; or the mechanisms that cause bottleneck discharge flows to change with varying O-D flows. These models therefore may not reliably predict system-wide queuing and vehicle delays induced by weaving bottlenecks over the course of a rush.

2.3. Empirical Observations of Weaving Bottlenecks

Though most of the previous studies failed to capture traffic details regarding weaving bottlenecks, there were two empirical studies that serve as exceptions. E. Kwon (1999) collected real data from six freeway weaving sections. The study did not verify that the sites were active bottlenecks. It did, however, report an interesting phenomenon: as weaving flows increase, F-R vehicles tend to perform their lane-changing maneuvers closer to the merge. Similar observations were made in the present study, where it was found that this lane-changing behavior influences both the activation of weaving bottlenecks, and their discharge flows.

R.L. Bertini (2004) used loop detector data to study a freeway weaving bottleneck with a metered on-ramp. The report noted that the activation of the weaving bottleneck was

[3] The term active denotes that a queue forms upstream while freely flowing traffic persists downstream

accompanied by discharge flow reductions. Bertini observed surges in on-ramp and off-ramp flows prior to the bottleneck activation, and conjectured that the bottleneck was triggered by vehicular conflicts between merging and diverging traffic.

Bertini further observed (on three different days) that reductions in on-ramp flow consistently coincided with bottleneck activations, and speculated that these reductions in ramp flows were constrained by queues on the freeway. Interestingly though, the on-ramp flows were only around 200 vph immediately prior to the bottleneck activations. This suggests that the on-ramp reductions were caused by reductions in demands, not by queues on the freeway. The recurrent pattern (reductions in ramp flows coinciding with bottleneck activations) implies that the reductions in ramp flows may be a causal factor of weaving bottlenecks; and this is consistent with findings from the present study.

2.4. Car-following Models with Optional Lane Changes

The present research approaches weaving from a microscopic perspective. To model microscopic traffic details on weaving sections, theories of driver lane-changing behavior developed by Laval (2006) and Menendez (2006) were adapted. Unlike other simulation models, these are parsimonious (they have a small number of parameters that can be readily observed in real traffic data.).

Laval formulated a multilane kinematic wave model with a hybrid structure; i.e., the model is macroscopic but lane changes are treated microscopically. According to this model, lane-changing maneuvers can create voids in traffic streams, and these voids can

travel forward and reduce bottleneck discharge flows. This model was not developed for weaving sections. Rather, it considers freeway sections away from diverges, where the main incentive for drivers to change lanes is to increase their speeds. Under dense traffic conditions, a lane-changing vehicle can behave as a moving-bottleneck in its destination lane while it accelerates to the speed prevailing in that lane. This disturbance can trigger lane changes among other vehicles. Findings of the present study indicate that similar lane-changing phenomena occur in weaving sections.

Laval's model was a starting point for work by Menendez who developed a microscopic car-following model with lane changes (detailed descriptions of this model are presented in the appendix.). The car-following component of the Menendez's model has three parameters calibrated to data based on three physical principles: vehicles' mechanical limitations (vehicles are constrained by their maximum acceleration and deceleration rates); safety (vehicles must be able to make a full stop at any time without crashing into vehicles in front); and driver comfort (vehicles are also limited by comfort constraints based on a simple linear car-following model (CF(L)) in Daganzo, 2004.). The model is discrete in time, but continuous in space. All drivers make decisions simultaneously. Additionally, there are two types of lane changes in the model:

i) optional lane changes generated by speed differences between two adjacent lanes

ii) mandatory lane changes generated by the activation of part-time High Occupancy Vehicle (HOV) lanes, or by the desire to enter/exit the freeway.

The Menendez model was tested at an on-ramp merge, a lane-drop bottleneck, and a

freeway section with an HOV lane. The model consistently reproduced real-world phenomena including discharge flow reductions at merge bottlenecks; the generation of oscillations created by a lane-drop bottleneck; and discharge flow reductions due to lane changes induced by the activation of a part-time HOV lane.

However, the Menendez model was not designed for weaving sections, and it describes only simplified mandatory lane-changing maneuvers; i.e., the model specifies that mandatory lane changes should be performed within a certain area (*a lane-changing cone*) of freeway sections, and the shape of this area is fixed regardless of traffic conditions (see section 4.1 for details). As a result, it cannot reproduce some of the findings of the present study, which will be shown momentarily. Therefore, the mandatory lane-changing component in Menendez's model will be enhanced and extended to capture these weaving phenomena.

CHAPTER 3. EMPIRICAL FINDINGS

This chapter describes the empirical study of two freeway weaving sites. The findings indicate that a high concentration of F-R maneuvers near the on-ramp triggered bottlenecks; and that discharge flow reductions occurred immediately thereafter. Bottleneck discharge flows subsequently varied in response to the F-R vehicles' lane-changing patterns; i.e., discharge flows increased (diminished) as F-R maneuvers occurred further from (closer to) the merge. Findings further indicate that these F-R lane changes, in turn, were influenced by the conditions in the auxiliary lane; i.e., F-R maneuvers migrated further from (closer to) the on-ramp as density in the auxiliary lane increased (decreased). The evidence follows. Section 3.1 presents empirical findings from the first study site. Section 3.2 shows that these findings were reproducible at a second study site. Section 3.3 summarizes the empirical findings from both sites.

3.1. Site 1: SR-55N, Santa Ana, CA

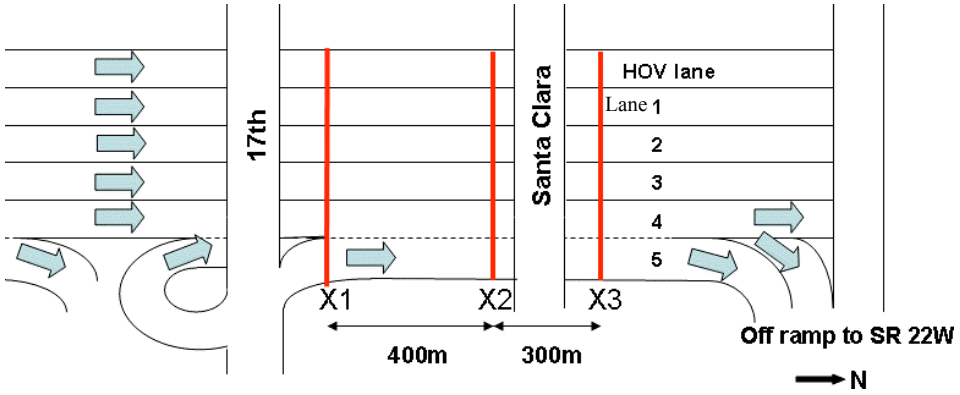

Figure 2. Study site, SR-55N

The first weaving study site, a stretch of northbound SR 55 in Santa Ana, California, is

shown in figure 2. There are two on-ramps from 17th street. These ramps are not metered, and were not queued during the three observation days (May, 16, 2005; May, 17, 2005; and August, 9, 2005). The median lane is reserved for HOVs. No vehicles entered or exited that lane within the segment labeled X1 and X3; the HOV lane was separated from the other general-purpose lanes over this length by means of solid painted stripes. There are in total 6 lanes, including the HOV lane. Those labeled 4 and 5 in the figure provide access to the off-ramp connector to State Route (SR) 22 west. There are two over-crossings (Santa Clara Ave. and 17th street), which offer suitable vantage points for videotaping traffic within the weave section. Multiple video cameras were installed on these over-crossings and detailed traffic data were extracted from the afternoon rush periods on the three observed days.

3.1.1. Details of Bottleneck Activation and Discharge Flow Reductions

Vehicle counts were measured at the locations labeled X1, X2, and X3, and cumulative count curves of these were constructed on an oblique coordinate system (O-curves), as shown in figure 3[4]. The slopes of the O-curves are the excess flows over a background flow, which is 9100 vph in the present case: high (low) slopes indicate high (low) flows. Moreover, the curves were constructed in such ways that superimposed curves indicate free flow traffic, and separated curves indicate delays between the measurement locations: the wider the separations, the longer the delays (see Cassidy and Windover,

[4] Since vehicles in the HOV lane were freely flowing and not affecting vehicles in other lanes, the former were not used for constructing the O-curves.

1995). All three curves in figure 3 were superimposed until 16:51 hrs, indicating that traffic was initially freely flowing. The curve at X1 started to diverge at this time from the curve at X2, indicating that delays and queuing arose between X1 and X2; i.e., the weaving segment became an active bottleneck at about 16:51 hrs. Note that the location of the bottleneck (between X1 and X2) indicates that the slow-down in the weaving section was not trigged by a queue spill-over from anywhere downstream, including the off-ramp.

Figure 3 also shows that the bottleneck's activation was accompanied by discharge flow reductions; flows dropped from 9865 vph to 8465 vph, a 14 percent reduction. Detailed analysis shown momentarily indicates that this diminished discharge flows (at 16:51 hrs) resulted from the concentration of disruptive F-R maneuvers near the on-ramp. To unveil this mechanism, the discharge flows in individual lanes 3, 4, and 5 are examined next.

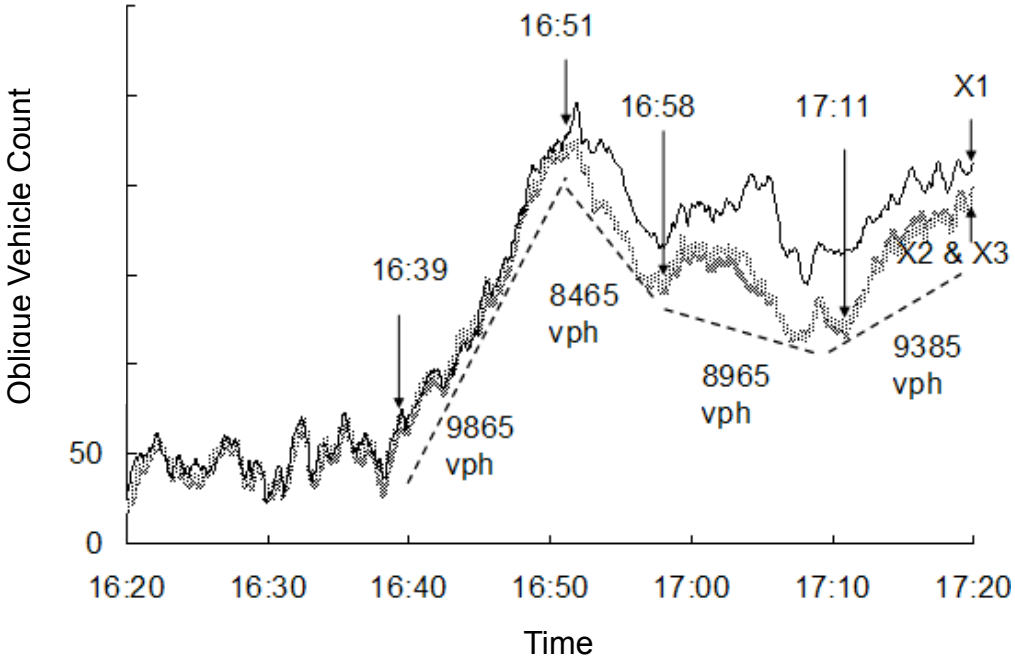

Figure 3. Oblique count curves at X1, X2, and X3, SR-55 N

3.1.2. Individual Lane Discharge Flows

Figure 4 shows separate O-curves for lanes 3, 4, and 5 that were measured at X2 during the period surrounding the bottleneck activation. The discharge flow reduction was first observed in lane 4 at 16:51:10; then in lane 5 at 16:51:22; and eventually in lane 3 at 16:51:46. Also note that after the initial flow reduction in lane 4, there was a short period (period (iii)) with a higher discharge rate (the cause of this increase will be presented in a moment.). For now, note the four periods characterized by distinct discharge flow in lane 4 (where the events began); these are labeled (i) ~ (iv) in figure 4. To understand the mechanism of these changes in discharge flows (reductions in the periods (ii) and (iv) plus increases in the period (iii)), vehicle trajectories in lane 4 are examined next.

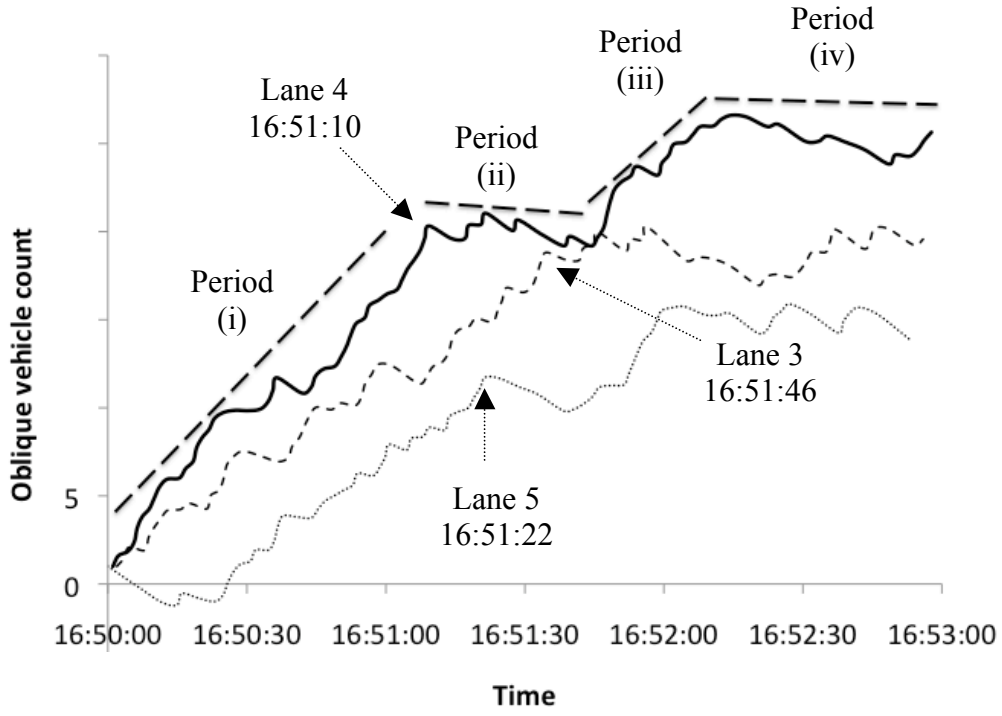

Figure 4. Discharge flows in individual lanes at X2, lanes 3, 4 and 5, SR-55N

3.1.3. Vehicle Trajectories in Lane 4

Vehicle trajectories in lane 4 are shown in figure 5. The periods (i) through (iv) are shown in this figure as well. The darker trajectories represent F-R vehicles that maneuvered from lane 3 to 4. Thin trajectories represent all the other vehicles, including F-R vehicles that did not perform the above-stated maneuvers. All vehicles represented by thin trajectories were traveling in lane 4 upon entering the weaving section, and those that disappear in the midst of figure 5 are vehicles that maneuvered out of the lane.

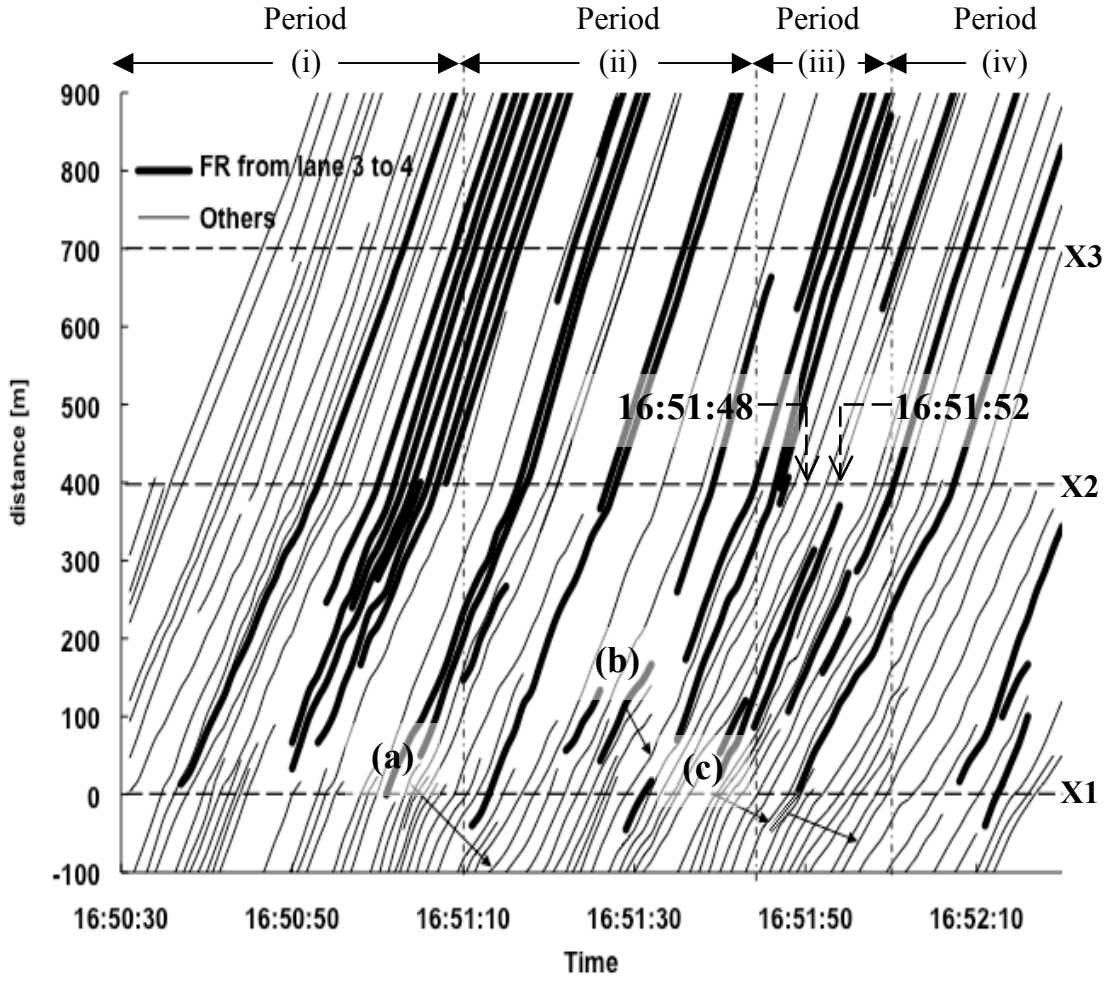

Figure 5. Trajectories of vehicles in lane 4, SR-55N

In period (i), a good many maneuvers out of lane 4 were observed near location X1. These left voids in the lane. These, however, were compensated by F-R vehicles that maneuvered from lane 3 to 4 at locations just downstream of X1, as shown by the thick trajectories. As a result, the lane 4's discharge flows at X2 did not decrease.

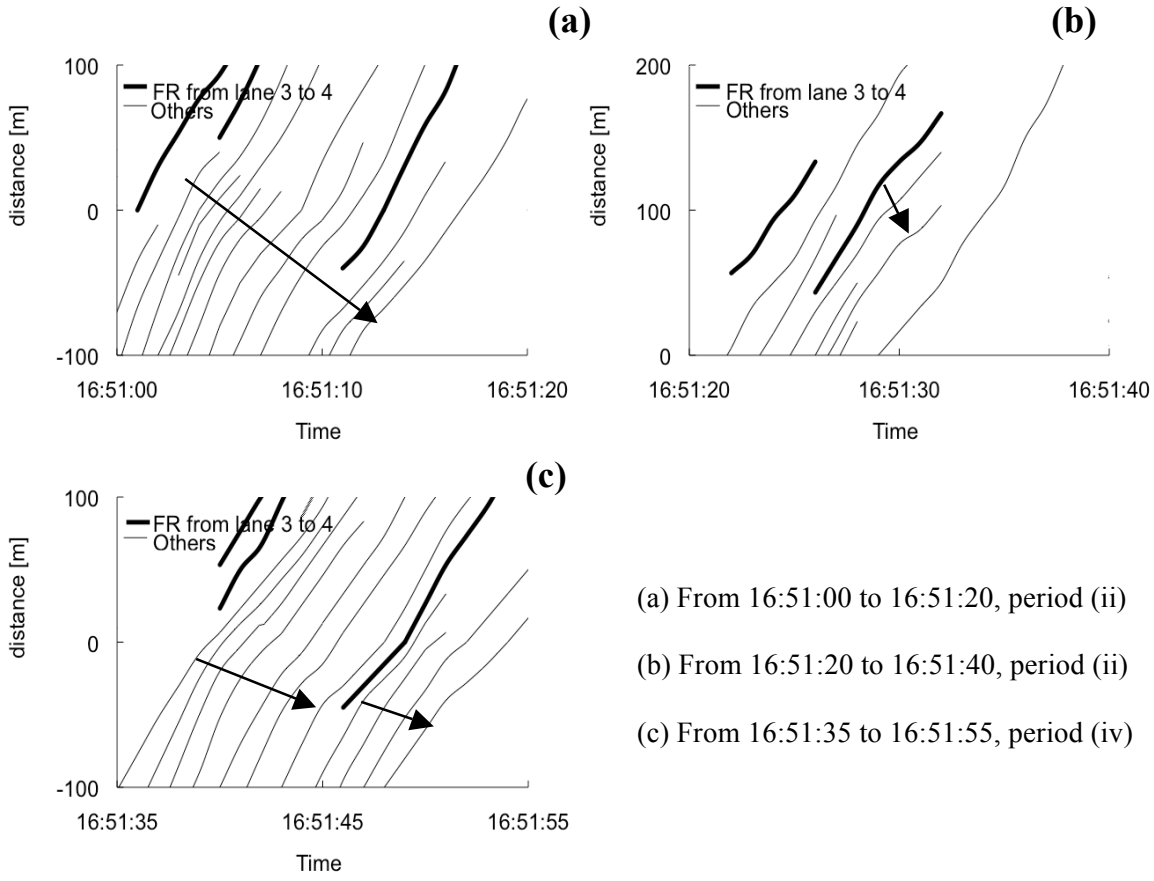

(a) From 16:51:00 to 16:51:20, period (ii)

(b) From 16:51:20 to 16:51:40, period (ii)

(c) From 16:51:35 to 16:51:55, period (iv)

Figure 6. Magnified vehicle trajectories in lane 4, SR-55N

During the low-flow periods (ii) and (iv), F-R vehicles maneuvering from lane 3 to 4 (dark trajectories) slowed the lane 4 vehicles behind them, generating deceleration waves. To see this, refer to the magnifications in figures 6a, b, and c. Figures 6a and b capture some of the lane 4 trajectories during period (ii), while figure 6c displays trajectories during period (iv). Notice from these figures how the lane entries of F-R vehicles (dark

trajectories) triggered deceleration waves; these waves are shown with arrows. Soon after being slowed, many vehicles maneuvered out of lane 4; as can also be seen in figures 6a and b. Most of these lane changers went to lane 5. As they did so, they created voids in lane 4. And because these lane-changing vehicles were traveling slowly, they also created voids in their target lane 5, which reduced discharge flows in that lane as well.

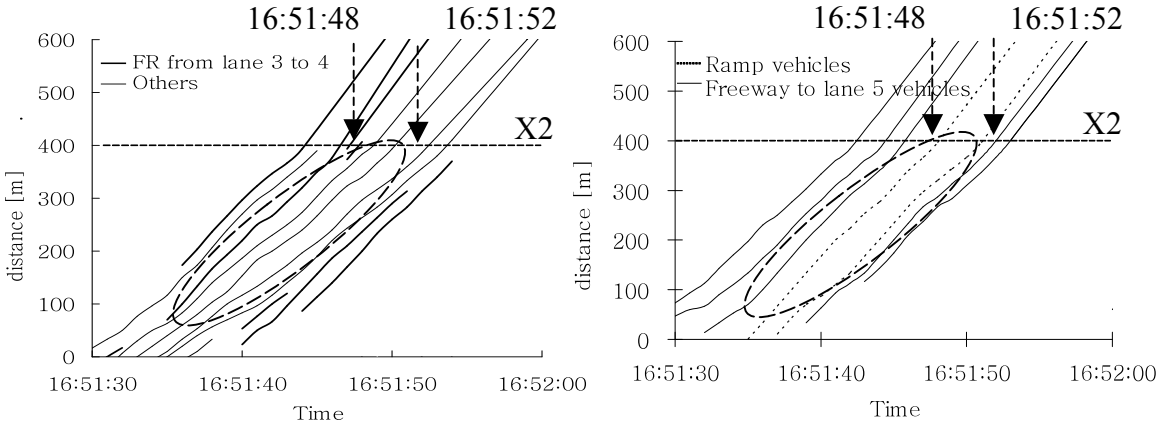

(a) Lane 4 (b) Lane 5

Figure 7. Vehicle Trajectories during period (iii) , SR-55N

Figures 7a and b show trajectories in lane 4 and lane 5 respectively during period (iii), a period of *higher* discharge flow as compared to the periods (ii) and (iv). Thin Trajectories in figure 7b represent F-R vehicles in lane 5, while dotted lines are vehicles from the on-ramp. Evidently, the discharge flows during period (iii) were high due to the presence of the two on-ramp vehicles in lane 5 (dotted lines). Note that these two vehicles passed location X2 at times 16:51:48 and 16:51:52. While they approached this location, there were no lane changes (from 4 to 5 and from 3 to 4), as can be seen by

viewing the encircled regions in figure 7a and b. It seems that the presence of these on-ramp vehicles reduced F-R drivers' motivation for maneuvering toward lane 5; and this reduced disruptive lane changes from 3 to 4. The discharge flows in lane 4 stayed high as a result. Further evidence of this key mechanism is presented next.

3.1.4. Effects of Mandatory Lane Changes on Discharge Flows

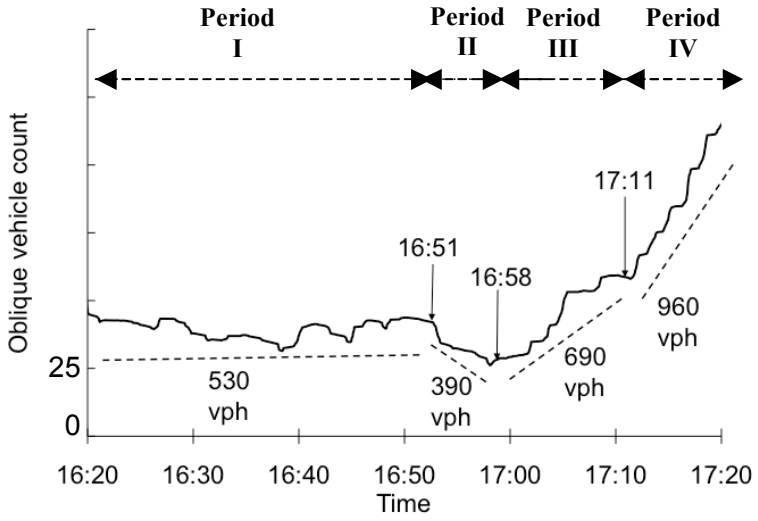

Figure 8. Oblique count curves of On-ramp flow, SR-55N

This section will discuss how bottleneck discharge flows depend on on-ramp flows. Figure 8 shows an O-curve of on-ramp counts for a 1-hr period that includes the period of bottleneck activation discussed in the previous section. The on-ramp flows decreased at 16:51 hrs (period II in figure 8), but increased at 16:58 hrs (period III) with a further increase at 17:11 hrs (period IV). Tellingly, these are the times when the weaving bottleneck's total discharge flows changed in the same direction, as shown in figure 3. Note how the bottleneck's initial discharge flow reduction at 16:51 hrs occurred when the

on-ramp flows decreased. Note too that at 16:58 hrs and 17:11 hrs, the bottleneck flows (figure 3) increased by amounts that exceeded the increases in on-ramp (figure 8). During these same latter two periods, there were no significant changes in the rate of F-R maneuvers, indicating that the changes in on-ramp flows were the cause for the observed changes in bottleneck discharge.

To further explore this causality, two mandatory lane-changing maneuvers are examined:

i) F-R maneuvers from lane 3 to lane 4

ii) R-F maneuvers from lane 5 to lane 4

Figures 9, 10, 11, and 12 show cumulative distributions of the locations of these two maneuvers during period I-IV, and over the segment from X1 to X2. Before the bottleneck activated at 16:51 hrs (period I), most of F-R maneuvers occurred near the on-ramp location X1. The solid curve in figure 9 shows that 50% (0.5 in y-axis) of the total F-R maneuvers were performed within 160 m of the on-ramp. Figure 11 shows that for the same period (I), 50% of total R-F maneuvers were performed within 140 m of the on-ramp.

However, when the bottleneck activated (period II), locations for the F-R lane changes (from lane 3 to 4) moved even closer to the on-ramp, even though lane 4 was the lane with the highest traffic density. Note from figure 9 the significant concentration of F-R lane-changing maneuvers near the on-ramp: 50% of these maneuvers took place within

130 meters from the ramp as shown with the dotted curve. This concentration near the merge resulted in vehicle slow-downs and produced the discharge flow reduction during the period, as previously shown in the previous section. Figure 11 shows that during the same period (II), mandatory R-F lane changes migrated further downstream (compare the dotted curve to the solid one). It is conjectured that the different migration patterns shown in figure 9 and 11 occurred because lane 5 always exhibited relatively low density and high speed; i.e., lane 5 became "attractive" to F-R and R-F vehicles in period II.

Consider now period III. The attractiveness of lane 5 was reduced when the on-ramp flows increased during period III; traffic in lane 5 became denser and travel time increased there. As a result, the traffic patterns in period III returned (approximately) to those in period I. Figures 10 and 12 show that the patterns (dash-dotted curves) from 16:58 hrs to 17:11 hrs are similar to those (solid curves) before 16:51 in figures 9 and 11. Reduction in the concentration of disruptive F-R maneuvers near the merge, therefore, resulted in the discharge flow increase at 16:58 hrs (period III) from 8465 vph to 8965 vph (figure 3), which is greater than the on-ramp flow increase from 390 vph to 690 vph (figure 8) [5].

Consider next period IV. The additional increase in on-ramp flows at time 17:11 hrs (period IV in figure 8) again reduced lane 5's attractiveness. Consequently, many R-F

[5] This outflow increase was caused by the reduction in the concentration of disruptive F-R maneuvers near the merge, not by a reduction in F-R maneuvers. The amount of mandatory F-R lane changes that took place between X1 and X2 remained the same, but increased downstream of X2 (from 154 vph to 234 vph).

maneuvers (the solid curve in figure 12) occurred further upstream as compared with previous time periods, as encircled in figure 12. In contrast, numerous F-R maneuvers (the solid curve in figure 10) took place further downstream, again reducing disruptive lane-changing maneuvers near the merge. Figure 10 also shows that the cumulative distribution of F-R maneuvers during the period IV became closer to a straight lane, indicating a more uniform distribution of F-R lane-changing maneuvers between X1 and X2 of the weaving section. The dispersion of disruptive F-R lane-changing maneuvers led to further increase in discharge flows at 17:11 hrs from 8965 vph to 9385 vph, greater than the increase in the on-ramp flows[6].

In summary, the data unveil the following mechanism. Reductions in on-ramp flows encourage F-R drivers to perform their maneuvers near the merge, and this concentration of disruptive F-R maneuvers near the merge triggers reductions in bottleneck discharge flows. Increases in on-ramp flows discourage F-R drivers to maneuver near the merge, and as a result bottleneck discharge flows increase. Further evidence of the relationship between on-ramp flows and bottleneck discharge rates are furnished for other days in the following section.

[6] Again, the cause of this increase was caused by the change in the distribution of F-R maneuvers, not by a reduction in F-R maneuvers. During this period IV, the amount of mandatory F-R lane changes between X1 and X2 did not change, but increased downstream of X2 (from 234 to 307 vph).

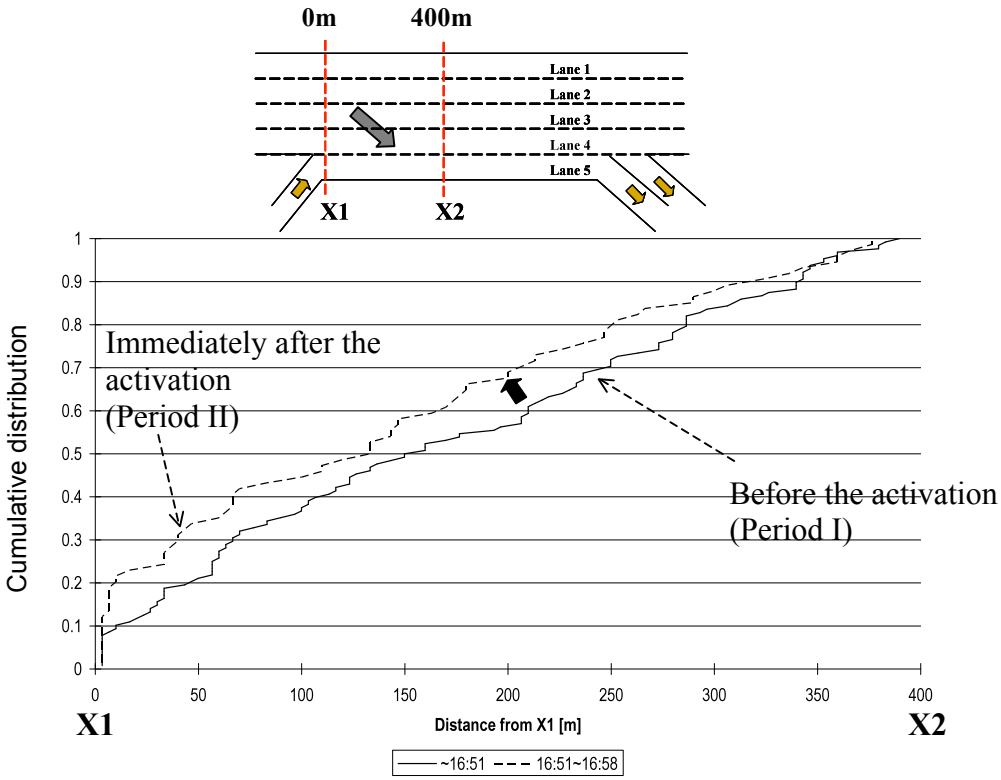

Figure 9. Cumulative distributions of F-R vehicles' lane changes from 3 to 4 before 16:58 hrs, SR-55N

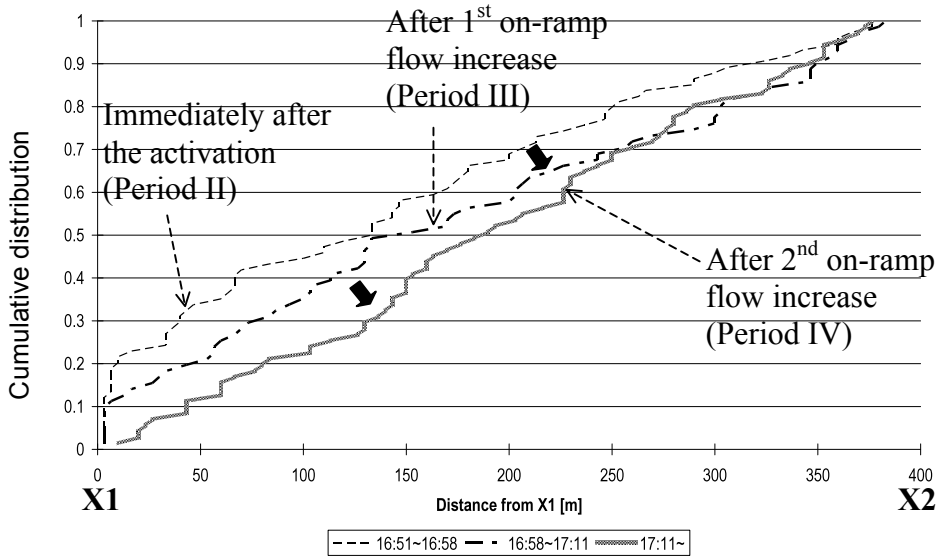

Figure 10. Cumulative distributions of F-R vehicles' lane changes from 3 to 4 after 16:51 hrs, SR-55N

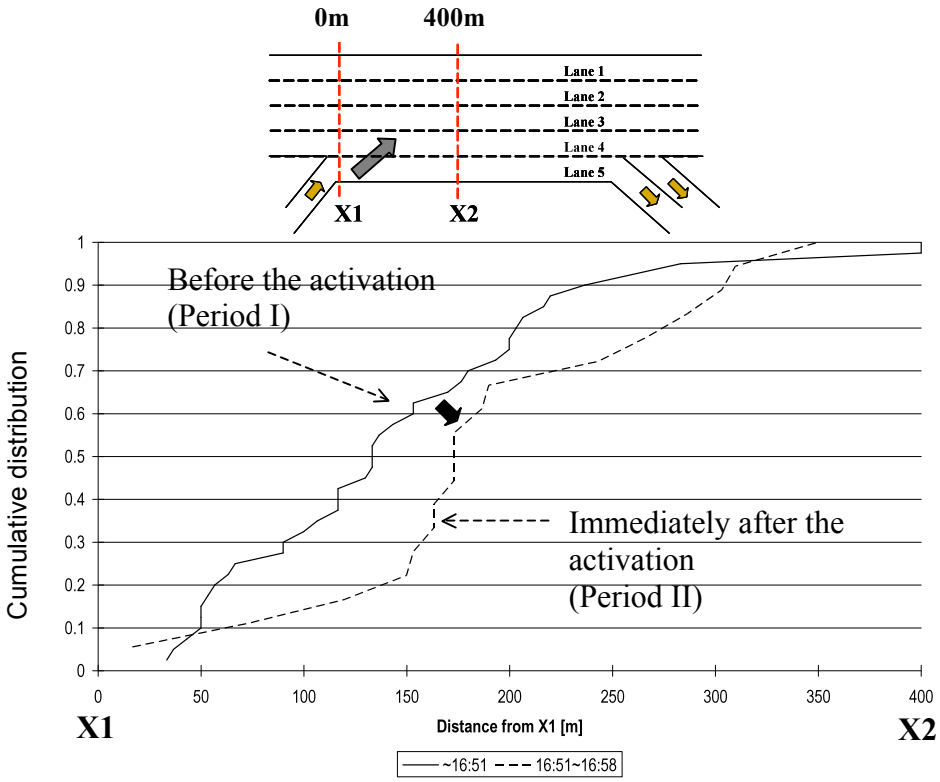

Figure 11. Cumulative distributions of R-F vehicles' lane changes from 5 to 4 before 16:58 hrs, SR-55N

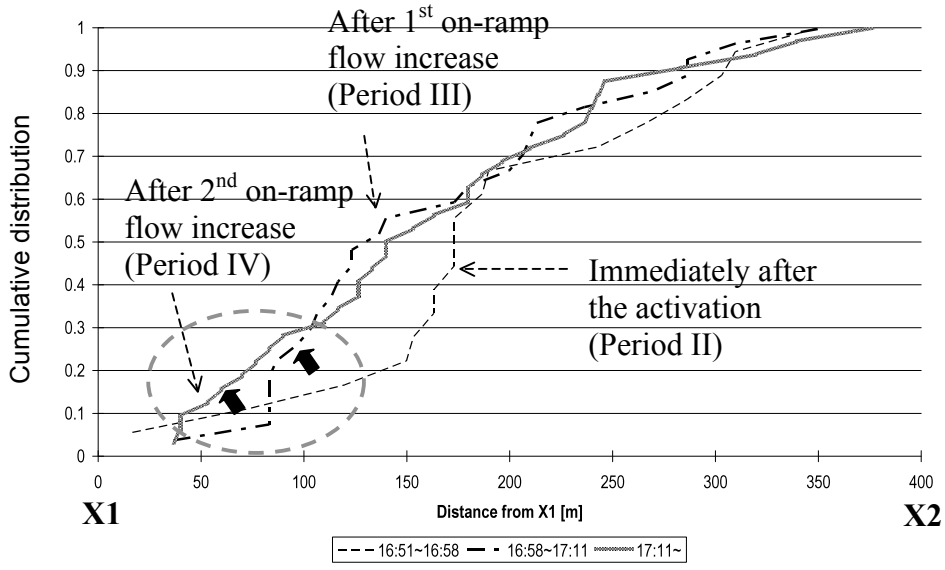

Figure 12. Cumulative distributions of R-F vehicles' lane changes from 5 to 4 after 16:51 hrs, SR-55N

3.1.5. Further Evidence of the relationship between on-ramp flows and bottleneck flows

O-curves of on-ramp flows and discharge flows were measured for two additional days, as shown in figures 13 and 14. These curves confirm that the observed mechanism is reproducible (see figures 3 and 8): the positive (negative) changes in on-ramp flows apparently reduced (increased) the attractiveness of the auxiliary lane among F-R drivers, and as a result discharge flows increased (diminished).

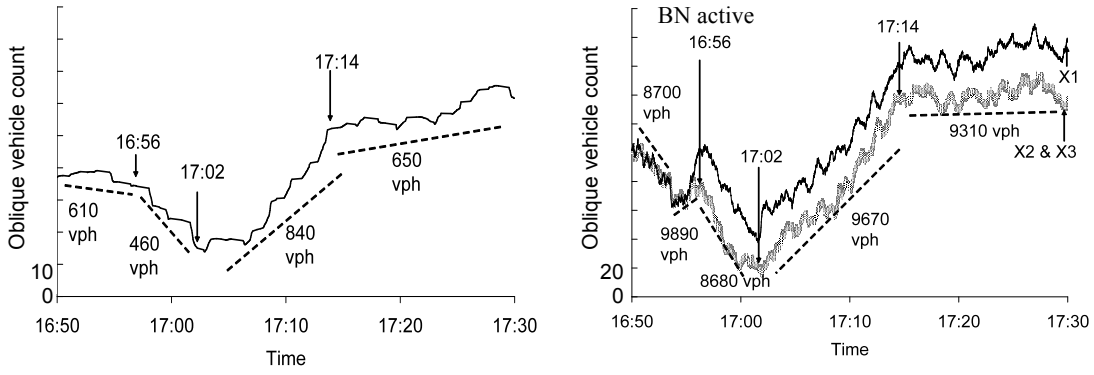

(a) On-ramp flow (b) Freeway at X1, X2, and X3

Figure 13. O-curves of on-ramp and freeway flows from 5/17/2005, SR-55N

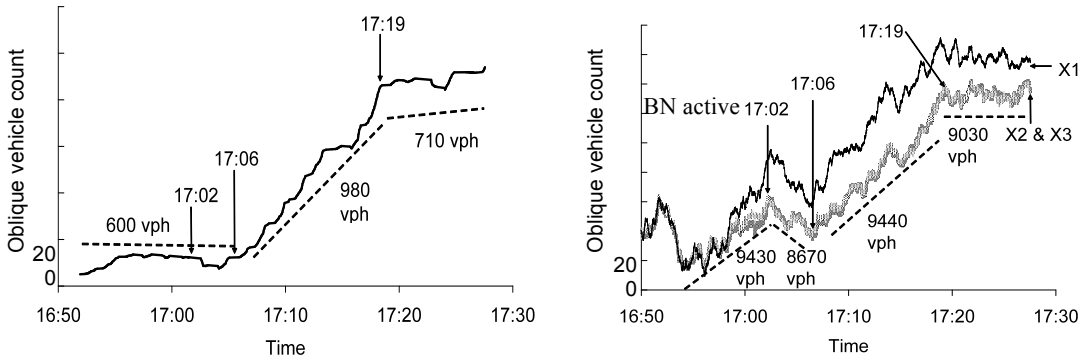

(a) On-ramp flow (b) Freeway at X1, X2, and X3

Figure 14. O-curves of on-ramp and freeway flows from 8/9/2005, SR-55N

Figures 13a and b show that when the on-ramp flows changed at 16:56 hrs, 17:02 hrs, and again 17:14 hrs, the total outflows changed in the same directions. Note that the bottleneck became active (figure 13b) when the on-ramp flows decreased at 16:56 (figure 13a). Note on another day shown in figures 14a and 14b, that when the on-ramp flows changed at 17:06 hrs and 17:19 hrs (figure 14a), further changes in the total outflow were observed (figure 14b). Note too that the bottleneck on this day became active at 17:02 without significant reductions in on-ramp flows. This activation was due to increased F-R demand.[7] The empirical results thus indicate that F-R lane changes became disruptive: i) when there are increased concentrations of F-R lane changes near the on-ramp merge triggered by reductions in on-ramp flows; or ii) when there are simply too many F-R lane changes, independent of the ramp flows.

Next, traffic data from another weaving study site with different geometry and different O-D demands will be examined to see if the observed mechanism is reproducible at this second site.

[7] At 17:02, the number of F-R lane changes from lane 3 to 4 between locations X1 and X2 increased from 548 vph to 951 vph

3.2. Site 2: I-210W, Pasadena, CA

To confirm the mechanism's reproducibility, we examine the stretch of westbound I-210 in Pasadena, CA, shown in figure 15. The on-ramp from Lake Ave was metered but rarely queued during the observation day. The median lane is reserved for High Occupancy Vehicle (HOV). The lane is separated from the other lanes by means of a solid painted stripe, and thus no vehicles entered, or exited the HOV lane between the locations labeled X1 and X3. No on-ramp vehicles from Lake Ave. were observed to use either off-ramp (to Marengo Ave. or I-210W). The two over-crossings (El Molino Ave. and Los Robles Ave.) offered suitable vantage points for videotaping traffic. Multiple video cameras were used to this end. Detailed traffic data were extracted from the morning rush period on June 28, 2002.

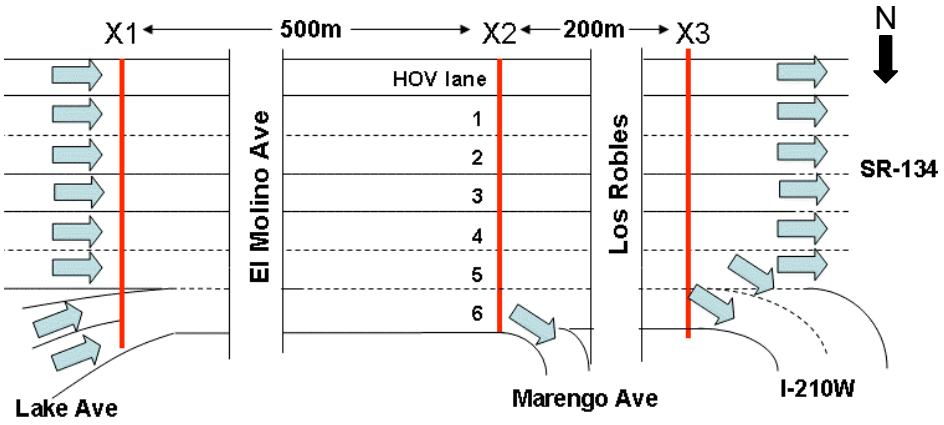

Figure 15. Study site, I-210W

3.2.1. Details of Bottleneck Activation and Discharge Flow Reduction

O-curves at locations X1, X2, and X3 were constructed for lanes 1 to 6 (excluding the

HOV lane) in the same manner described previously; see figure 16. Off-ramp flows observed at Marengo were added to the curve at X3 to maintain the conservation of flows. These O-curves reveal that the weaving segment between X1 and X2 became an active bottleneck accompanied by a discharge flow reduction at 6:54 hrs. Discharge flows dropped from 11100 vph to 10200 vph, an 8 percent reduction. When the bottleneck became active, no changes (reductions) in on-ramp flows were observed. However, F-R lane changes from lane 4 to 5 increased (from 521 vph to 962 vph) for a 3-min period beginning at 6:54 hrs. Since these observations are qualitatively consistent with those of the previous (see figures 14a and 14b), this is a clue that the diminished discharge (at 6:54 hrs) resulted from increases in disruptive F-R maneuvers. The discharge flow increase at 6:57 for 2 minutes was caused by reductions (fluctuations) in both the on-ramp and F-R flows; while the discharge flow reduction at 7:07 was triggered by a reduction in on-ramp flows. Evidence of this mechanism will be presented next.

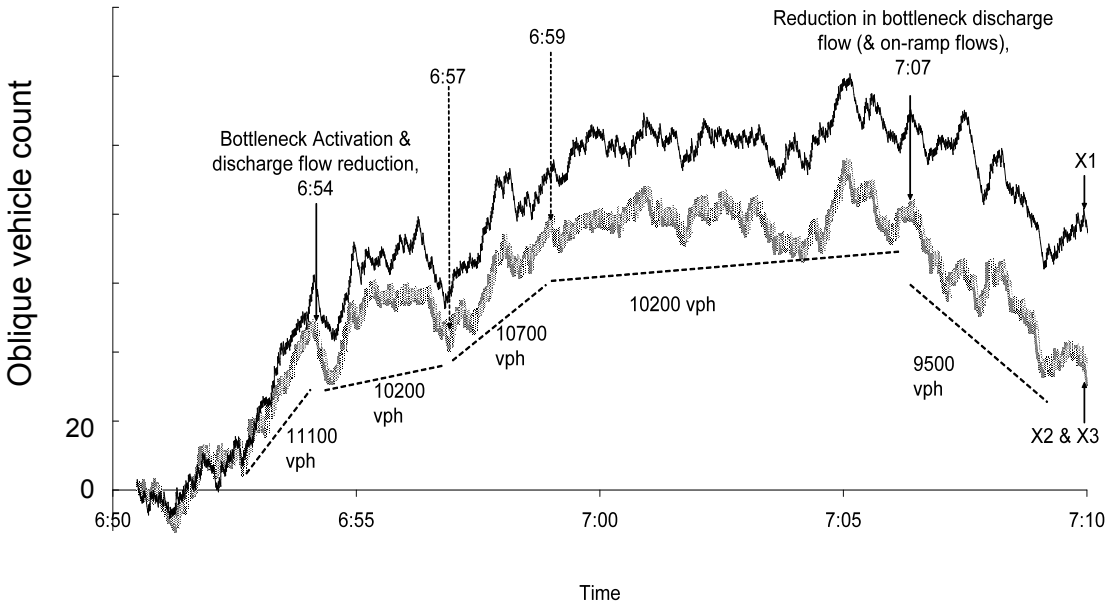

Figure 16. Discharge flows in individual lanes at X2, lanes 3, 4 and 5, I-210 W

3.2.2. Discharge Flow Changes Due to Mandatory Lane Changes

Lane-changing patterns previously presented in section 3.1.4 were observed at the present site as well, thus confirming the disruptive effects of F-R maneuvers. Figure 17 shows the O-curve of on-ramp flows. It shows that a reduction in this flow occurred at 7:07 hrs. Tellingly, this is the time when the weave bottleneck's total discharge flows decreased (see again figure 16). Two mandatory lane-changing maneuvers are examined between locations X1 and X3 to confirm the causal relation between the changes in both the on-ramp flows and the bottleneck discharge flows:

i) F-R maneuvers (destined to either the Marengo Ave. or the I-210W off-ramp) from lane 4 to lane 5

ii) R-F maneuvers from lane 6 to lane 5

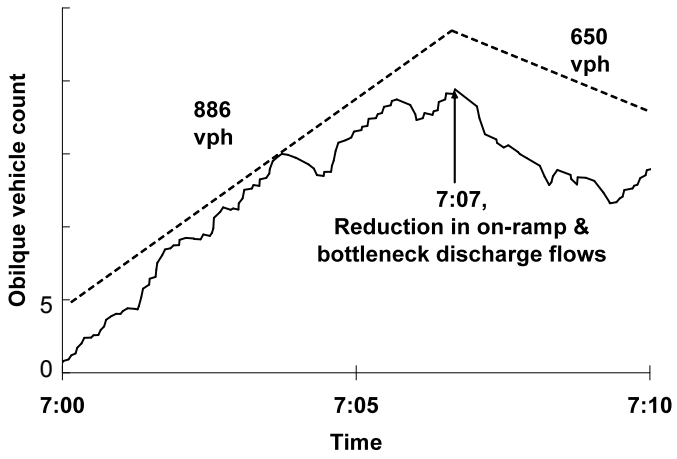

Figure 17. Oblique count curves of On-ramp flow, I-210W

Figures 18 and 19 show cumulative distributions of the locations of these two maneuvers during three distinct periods: before bottleneck activation at 6:54 hrs; the period after the

activation extending to the reduction in on-ramp flows at 7:07 hrs; and the period after 7:07 hrs. For now, this middle period excludes all data measured from 6:57 hrs to 6:59 hrs, the 2-min period when reductions in both on-ramp and F-R demands created a short-term increase in bottleneck discharge flows (see figure 16). Details concerning the F-R and R-F maneuvers during this 2-min period will be presented momentarily.

The thick solid curve in figure 18 shows that before the bottleneck activated at 6:54 hrs, 50% of total F-R maneuvers were performed within 340 m of the on-ramp. As regarding the R-F maneuvers during this same time, the thick solid curve in the lower figure, figure 19, shows that 50% of these were performed within 180 m of the on-ramp.

The distributions of these two maneuvers changed in opposite directions after the bottleneck became active at 6:54 hrs: F-R lane changes migrated further upstream, while their R-F counterparts migrated further downstream. The dotted curve in figure 18 shows the distribution during the middle period; note how the dotted curve lies above the thick solid one (before the activation at 6:54 hrs) in the figure. The concentration of these disruptive F-R maneuvers nearer the on-ramp merge resulted in the discharge flow reduction during this period. During the same period, mandatory R-F lane changes migrated further downstream (see the dotted line in figure 19). It is conjectured that these observed lane-changing patterns emerged because lane 6 always exhibited lower densities due to low on-ramp flows during the period. Thus, the lane was attractive to both R-F vehicles (which stayed longer in the lane) and F-R vehicles (which entered the lane sooner).

Notably, when the on-ramp flows decreased at 7:07 hrs, the thin solid line in figure 18 shows that F-R lane changes migrated even further upstream. At the same time, R-F lane changes migrated yet further downstream; note from figure 19 how the thin solid line lies below its dotted counterpart. Again we see the familiar lane-changing pattern induced by a reduction in on-ramp demands. Note from figure 16 how this pattern that emerged after 7:07 hrs was accompanied by a discharge flow reduction.

We now turn our attention to the period with the short-term reductions in both the on-ramp demands (that dropped from 935 vph to 650 vph); and the corresponding reductions in F-R demands (that decreased from 2370 vph to 1930 vph) during the 2-min period from 6:57 hrs to 6:59 hrs). These decreases in demands were accompanied by an increase in total discharge flow, as shown in figure 16. As a result, lane-changing patterns during this 2-min period were similar to those before the bottleneck activation. Figures 20 and 21 show that F-R and R-F lane-changing patterns during this 2-min period (dashed curves) were similar to those measured prior to the bottleneck's activation (thick solid curves). As a result of these similar lane-changing patterns, discharge flows during the 2-min period were similar to those measured prior to the bottleneck's activation (see figure 16).

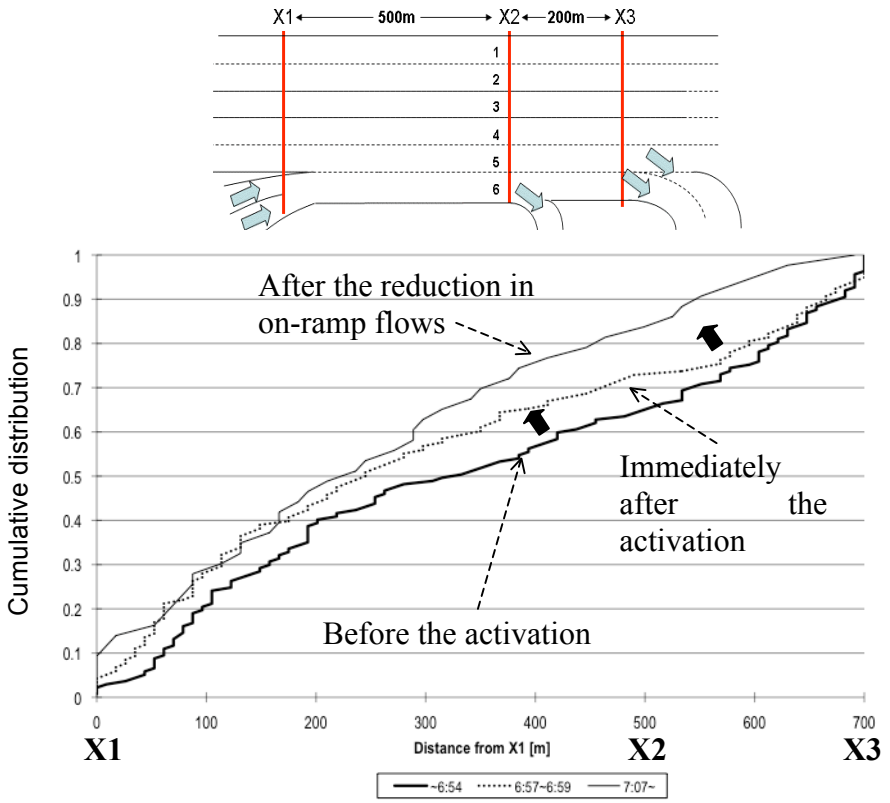

Figure 18. Cumulative distributions of F-R vehicles' lane changes from 4 to 5, I-210W

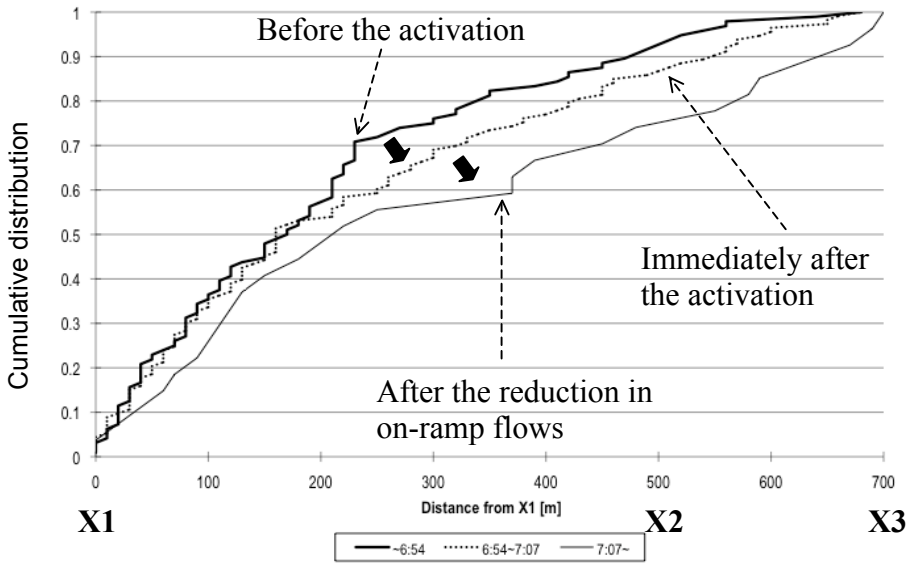

Figure 19. Cumulative distributions of R-F vehicles' lane changes from 6 to 5, I-210W

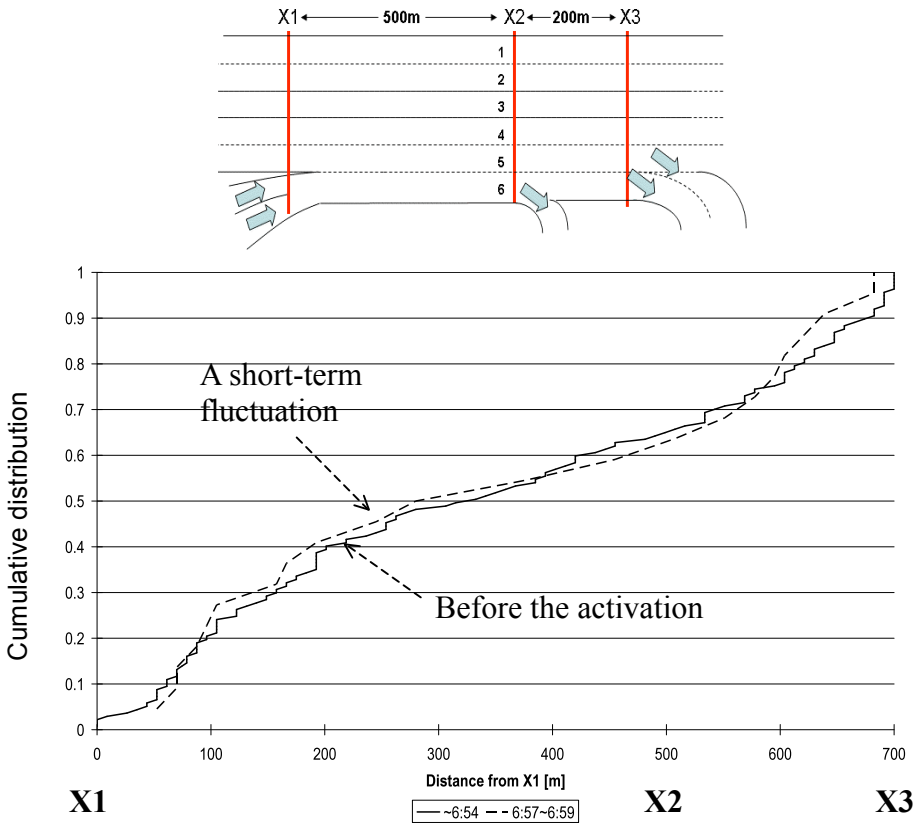

Figure 20. Cumulative distributions of F-R vehicles' lane changes from 4 to 5 between 6:57 hrs and 6:59 hrs, I-210W

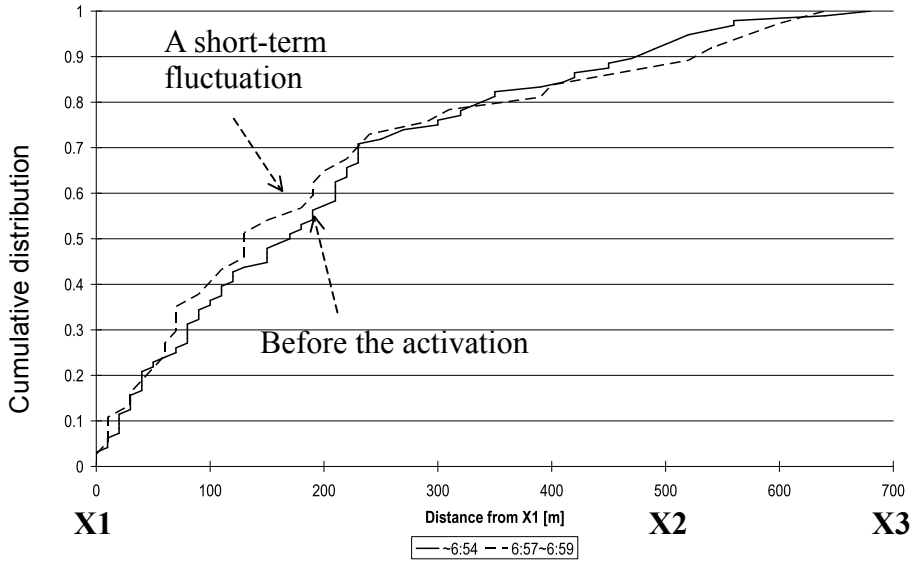

Figure 21. Cumulative distributions of R-F vehicles' lane changes from 6 to 5 between 6:57 hrs and 6:59 hrs, I-210W

3.3. Summary of Empirical Findings

The findings indicate that bottleneck activations at both weaving sections were triggered by disruptive F-R lane changes. These F-R lane changes became disruptive: i) when there were increased concentrations of F-R lane changes near the on-ramp merge triggered by reductions in on-ramp flows; or ii) when there were simply too many F-R lane changes, independent of the ramp flows. As a result, discharge flows in both weave study sites varied in response to the *distributions* of F-R maneuvers. Findings further indicate that the distributions of these lane changes, in turn, were influenced by the conditions (i.e., relative densities) of the weaving sections' auxiliary lanes. On-ramp flow reductions increased the attractiveness of the auxiliary lanes, thus motivating F-R drivers to perform their maneuvers nearer the on-ramp (fewer maneuvers downstream). This state of affairs produced the discharge flow reductions. In contrast, increases in on-ramp flows reduced the attractiveness of the auxiliary lanes, reducing the concentration of disruptive F-R maneuvers near the on-ramp (with more maneuvers occurring downstream). These reductions in disruptive maneuvers led to discharge flow increases.

The next Chapter presents a theoretical model based on the described mechanism and the model is tested with the traffic data at the two study sites.

CHAPTER 4. THEORETICAL MODELLING: MICROSIMULATION

This Chapter presents the car-following and lane-changing model adapted from *Menendez (2006)* to predict the observed mechanisms that activate bottlenecks in weaving sections and trigger changes in discharge flows. The model is tested with data from the two study sites, but data from only one of the sites (SR-55N) are used to estimate model parameters. The details of the new model will be described next. Test results will be presented in section 4.2.

4.1. Model Formulation

The model refined here, like the one originally developed by Menendez (summarized in section 2.4 and Appendix A), captures both the vehicle car-following and lane-changing processes. The model is discrete in time, but continuous in space such that it calculates the locations of individual vehicles over a stretch of freeway for every simulation interval. All drivers make decisions simultaneously, as in the original model.

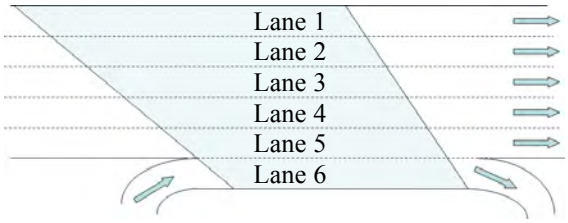

Figure 22. The original model's lane-changing cone for weaving sections

The original model assumes that the decisions of when to perform mandatory lane-

changing maneuvers are based on the number of lanes that the vehicle must cross and the remaining distance to the destination. When used to describe F-R vehicles in a weaving section, the original model assumes that once these vehicles enter the cone shown in figure 22, they try to change lanes by searching for a sufficient gap in the adjacent right lane.

To better emulate the weaving mechanisms observed in the present study, the adapted model uses a revised description of mandatory lane change behavior. This additional feature is the focus of the theoretical work presented next.

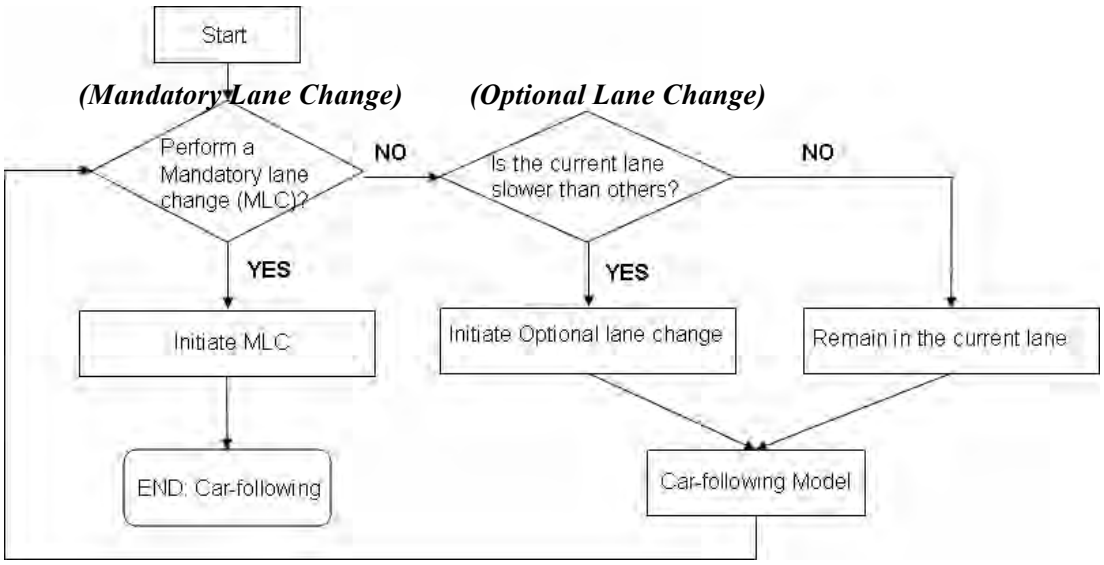

Figure 23. Flowchart of the adapted model

A flowchart of the adapted model is shown in figure 23. It includes a Logit model to determine the probability that each driver first attempts a mandatory lane change, P_{MLC}, at

a given simulation interval, t (the diamond labeled (Mandatory Lane Change) in figure 23).[8] The formulation for the P_{MLC} for each driver and each time interval is:

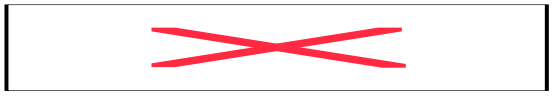

[1]

Where β_0, β_1, β_2, and β_3 are the parameter estimates, and the three variables x_1, x_2, and x_3 are described below.

The first variable, x_1, is a proxy for the difference in densities between a driver's current lane and the right-most lane: it is the difference in the vehicle accumulations between these two lanes, as measured over a 100-m long stretch extending from the driver's current position.[9] Note that if a driver is upstream of the weaving section (where there is no auxiliary lane), the right-most lane is lane 5 (see figure 22). If the driver is within the weaving section, then lane 6, the auxiliary lane, is the right-most lane.

The second variable, x_2, is an inverse of a vehicle's remaining normalized distance to the diverge; i.e., it is the length of the weaving section divided by of the vehicle's distance from the end of the weave; and the variable is normalized so that the parameter β_2 (in the

[8] The choice of the Logit model, instead of a more complex discrete choice model such as the random parameter model, was to minimize the number of parameters. Only those parameters conjectured from the observed mechanism are included in this Logit model.

[9] No existing decision models for mandatory lane changes consider this difference as an explanatory variable, though the empirical findings of this study indicate that this difference plays an important role.

equation [1]) estimated for one site may be generalized across sites. Note that as the vehicle's distance to the end of the weave approaches 0, the variable, x_2, becomes infinite, forcing P_{MLC} = 1. This reflects a driver's increased motivation to perform her mandatory lane change maneuvers as she moves closer to the downstream end of the weaving section.

The third variable, x_3, is the number of lanes that must be crossed to finish a mandatory lane change maneuver. This reflects a driver's propensity to attempt lane-changing maneuvers early if she is required to maneuver through multiple lanes.

Once the driver decides to perform a mandatory lane change (when a Bernoulli trial of P_{MLC} is a success in the simulation process), she continues to try to change lanes for every time interval in the simulation based on the car-following algorithms of the original model. If these attempts fail after a certain elapsed time ψ, the driver reduces her speed or a cooperating vehicle in the target lane makes space for her by reducing its own speed.

Optional lane change maneuvers are generated in the refined (and original) model when traffic in a driver's current lane is moving slower than in adjacent lanes (the second diamond labeled (Optional Lane Change) in figure 23). The car-following component of the adapted model also follows the logic developed by Menendez.

4.2. Parameter Estimation

To estimate the β in the equation [1], parameter values for car-following and optional lane change were taken from the Menendez's model. Table 1 provides descriptions and values of these parameters. More detailed descriptions of these parameters can be found in *Menendez (2006)*.

Parameter	Description	Value
u	Free-flow speed	70 mph
s_{jammed}	Jammed spacing	20 ft
r	Dimensionless proxy for deceleration rate	1
a_U	Acceleration rate	10 $ft/\sec^2$
w	Backward wave speed	14 mph
ϕ	Sensitivity to relative differences in speed between adjacent lanes for optional lane changes	4 sec
ψ	Cooperation initiation time for mandatory lane changes	5 sec

Table 1. Parameters from the original model for weaving

A few additional assumptions were made for estimating the β. It was assumed that during congested periods, drivers who decide to perform lane changes may delay their maneuvers due to lack of sufficient gaps in the target lane. Therefore, data during congested periods were not used to estimate the parameters for the equation [1]. In contrast, it was assumed that locations of lane changes made during free-flow states mark the locations where drivers made decisions.

In light of these assumptions, $\boldsymbol{\beta}$ were estimated using those vehicle trajectories from SR-55N (described in section 3.1.4) that were measured *prior to the bottleneck activation* (during free-flow states). Variables x_1, x_2, and x_3 were measured from these trajectories at *one-second* intervals. Since in the model, individual drivers make decisions every s*imulation interval* (not one second), linear interpolations of the measured $\boldsymbol{x}$ were applied to make the data compatible with the simulation.

The dataset contains 1512 observations of vehicle locations (specified at the intervals used in the simulation). These came from 310 mandatory lane changes made by numerous drivers. Maximum log-likelihood estimation was applied to these data to estimate the $\boldsymbol{\beta}$ in the equation [1], and the estimated values are shown in table 2.

Parameter	Description	Value
β_0	Constant	-8.0
β_1	Density difference	0.9
β_2	Inverse of normalized distance	6.3
β_3	Number of lanes to be crossed	1.2

Table 2. Estimated values of the parameters

The results of the simulation tests performed with the model are described below.

4.3. Model Testing

The model with its estimated $\boldsymbol{\beta}$ was applied to the two study sites. In section 4.3.1, model predictions were compared with empirical data at site 1 (SR-55 N). In section

4.3.2, the transferability of the parameter estimates was tested for site 2 (I-210 W); i.e., the β estimated for site 1 were used to make predictions and these were compared with observations from site 2. At both sites, the model was found to reproduce qualitatively the observed phenomena. Although the empirical results were previously presented in Chapter 3, some of them are re-presented in the present section for the reader's convenience.

4.3.1. Simulation Results for Site 1, SR-55 N

The input data for the simulations of site 1 consisted of on-ramp demand (R-R and R-F) and upstream freeway demand (F-F and F-R). The on-ramp was not queued during the observation periods, so the time-varying on-ramp demands were the on-ramp flows measured from videos. However, traffic in the upstream freeway segments was queued when the bottleneck became active, and thus upstream freeway demands were hidden. To resolve this issue, freeway demands prior to the bottleneck activation were used for the whole period, even after the bottleneck became active in simulation. Once the simulated queues propagated to the upstream boundary of the weaving area, the simulation model assigned incoming vehicles values of speed and spacing suitable for queued conditions.

The model was found to qualitatively replicate the site's observed O-curves (i.e. the bottleneck's activation time and the changes in its discharge flows); and the cumulative distributions of lane changes over space. Figure 24a re-presents the observed O-curves (at site 1; May, 16, 2005) and figure 24b displays O-curves predicted by the adapted model. By comparing these two figures, we see that the model accurately predicted the

bottleneck activation time, the times when the discharge flows changed, and the directions of these flow changes. Figures 25 and 26 show observed and simulated cumulative distributions of F-R lane changes from 3 to 4 during the time periods marked by distinct discharge flows. Figures 27 and 28 show these cumulative distributions for the R-F maneuvers. Note that the figures labeled (a) present observed data, and that those labeled (b) present simulated curves. Visual comparisons of a figure (a) with its counterpart (b) show that the model qualitatively replicates the observations within at most 500 vph differences: the observed and simulated cumulative distribution curves moved in the same directions from one time period to the next. And consistent with the observations, the upstream (downstream) migration of F-R maneuvers consequently decreases (increases) bottleneck discharge flows.

The model predicted similar trends for F-R vehicles on the upstream freeway segment, as they approached the weave area. These simulated results are consistent with the conjecture drawn from the empirical observations: during congested periods, F-R drivers try to minimize their delays by staying longer in lane 3 since densities were lower (and speeds are higher) in that lane as compared with lane 4. Once these drivers pass the on-ramp where the auxiliary lane (with lower densities and higher speeds due to low on-ramp flows) begins, F-R drivers minimize their delays by promptly initiating maneuvers to lane 4, and then to the auxiliary lane soon thereafter. It seems that this driver behavior lies in the heart of the mechanisms that trigger bottleneck activation and subsequent changes in discharge flows.

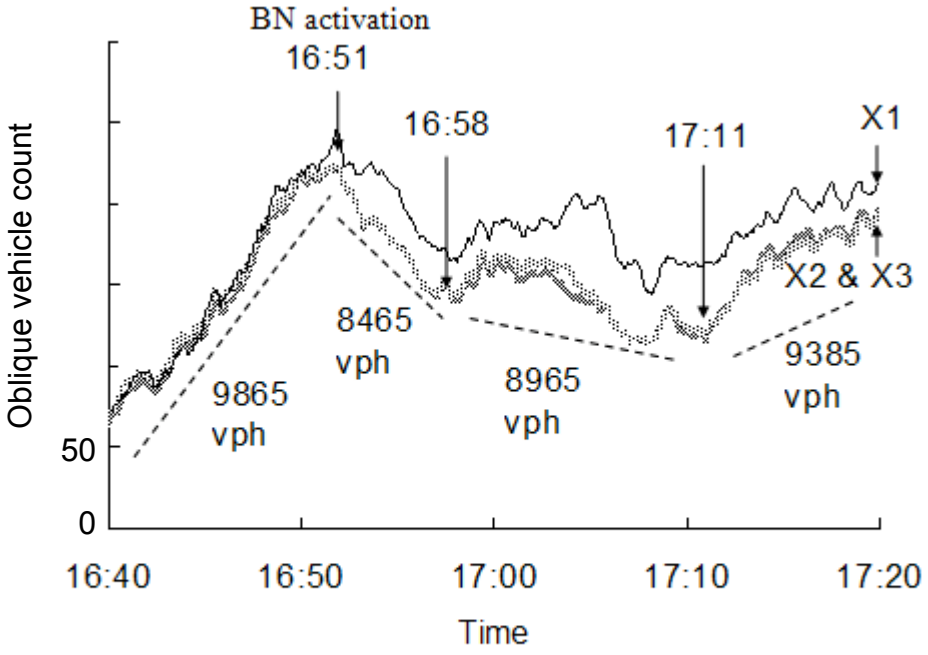

(a) Observed Curves

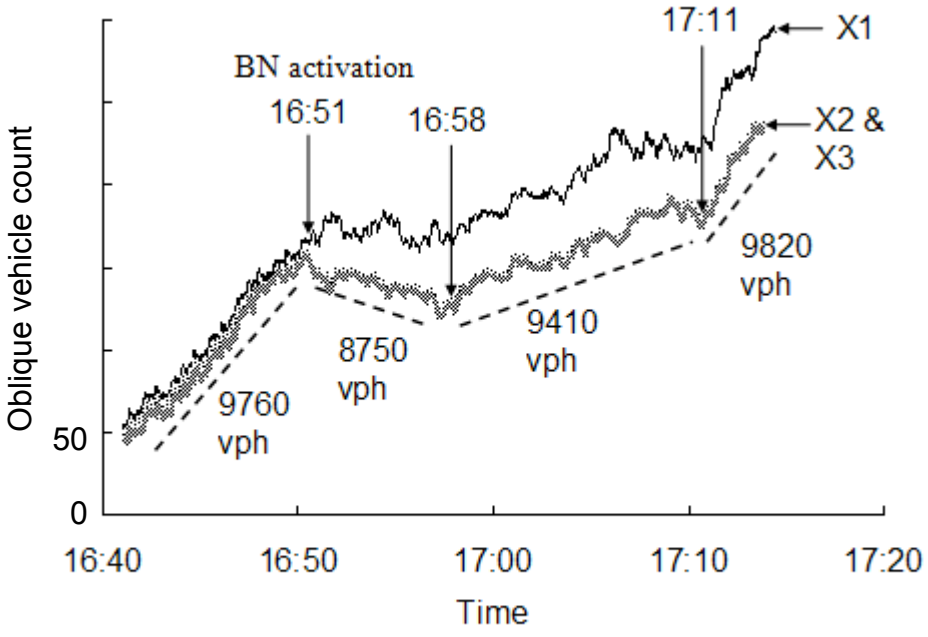

(b) Simulated Curves

Figure 24. Comparison of oblique count curves at X1, X2, and X3, SR-55 N

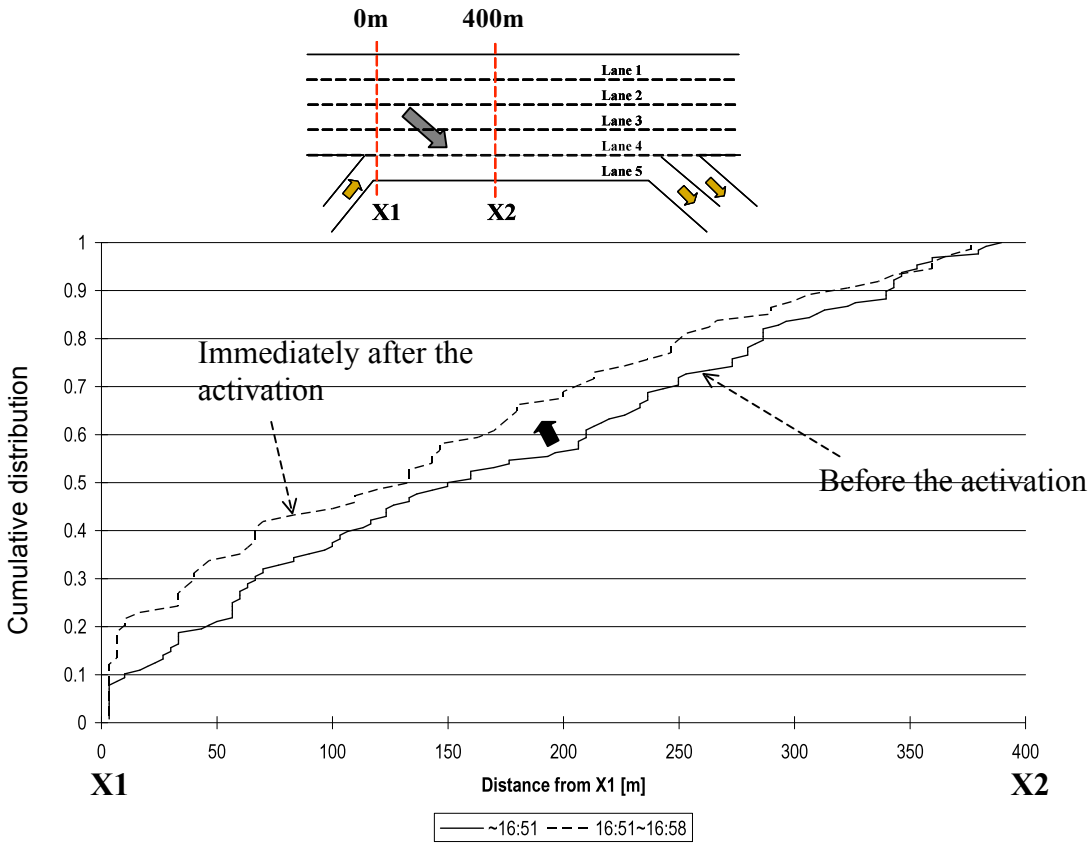

(a) Observed

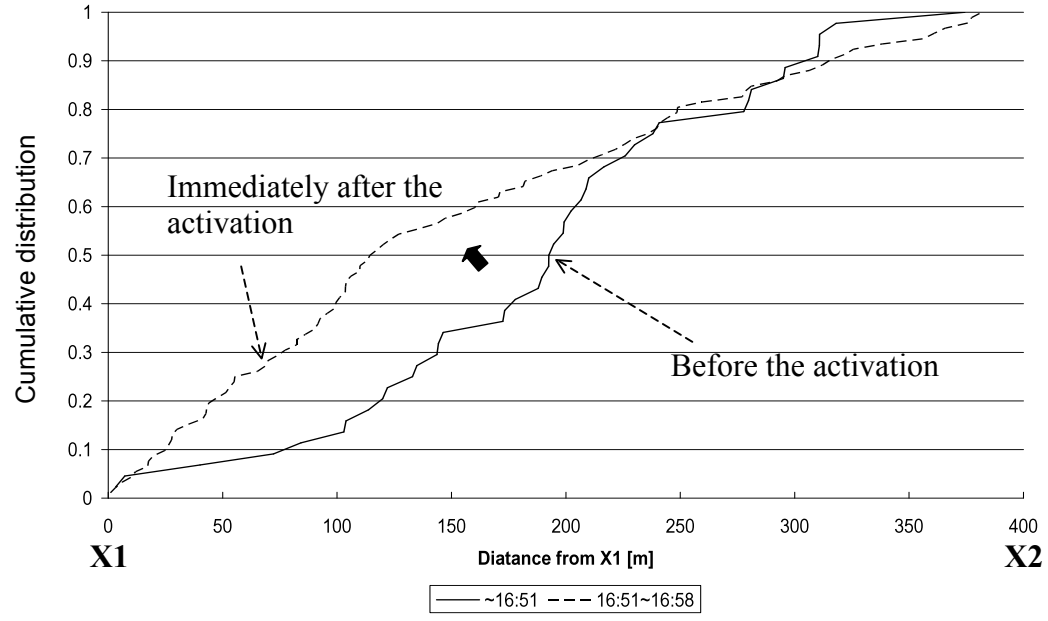

(b) Simulated

Figure 25. Comparison of cumulative distributions of F-R vehicles' lane changes from 3 to 4 before 16:58 hrs, SR-55N

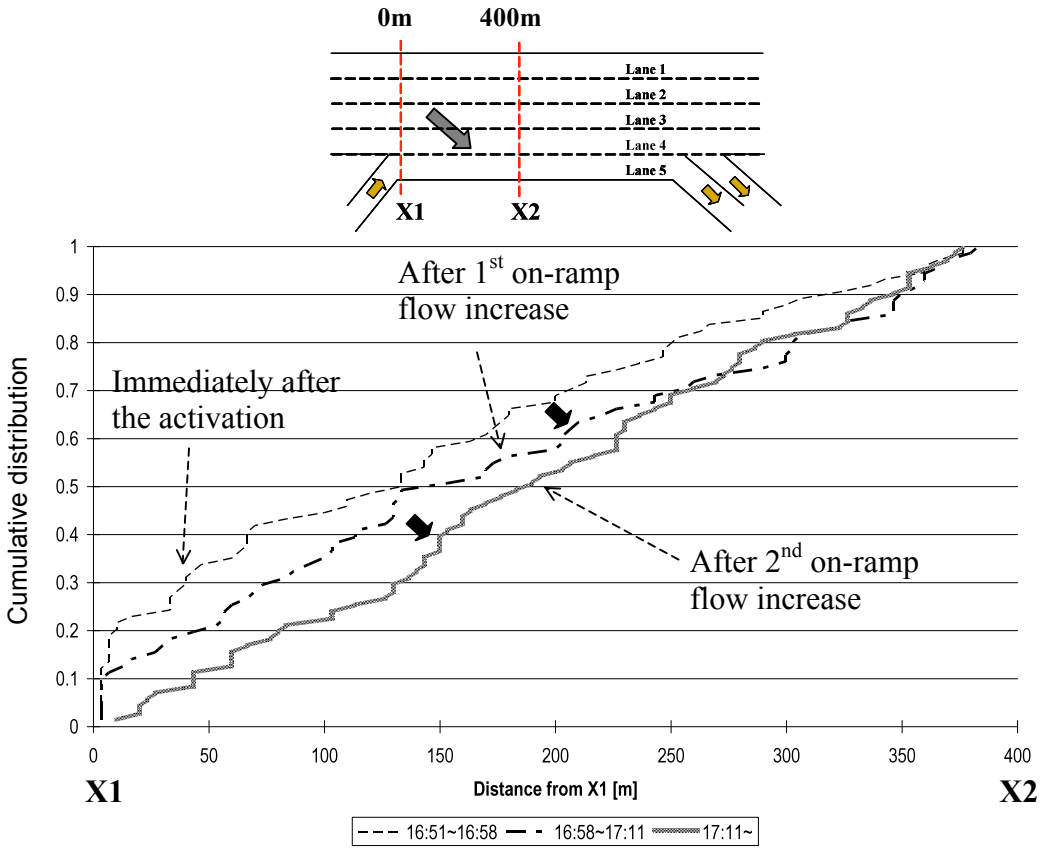

(a) Observed

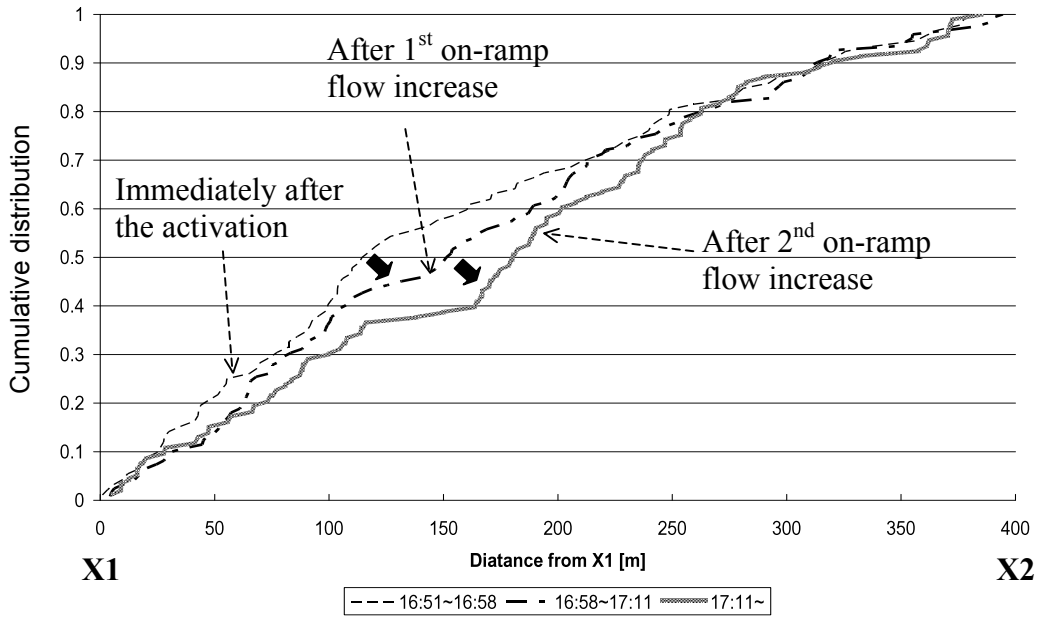

(b) Simulated

Figure 26. Comparison of cumulative distributions of F-R vehicles' lane changes from 3 to 4 after 16:51 hrs, SR-55N

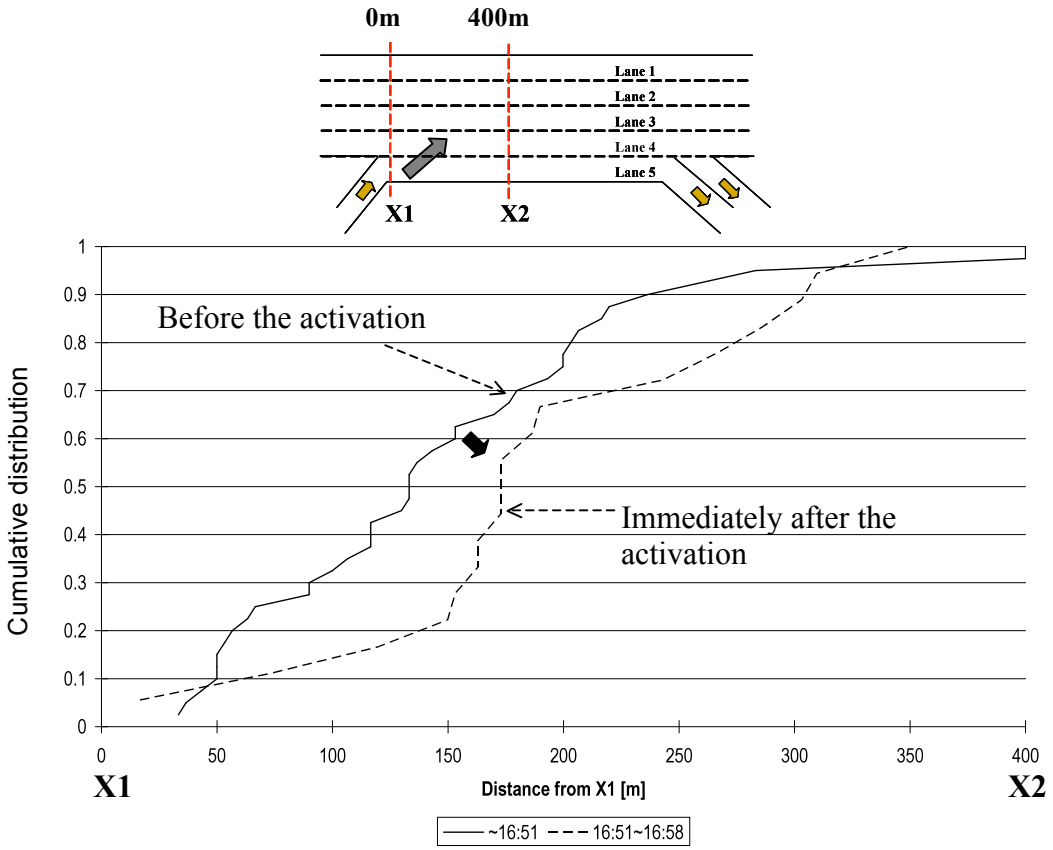

(a) Observed

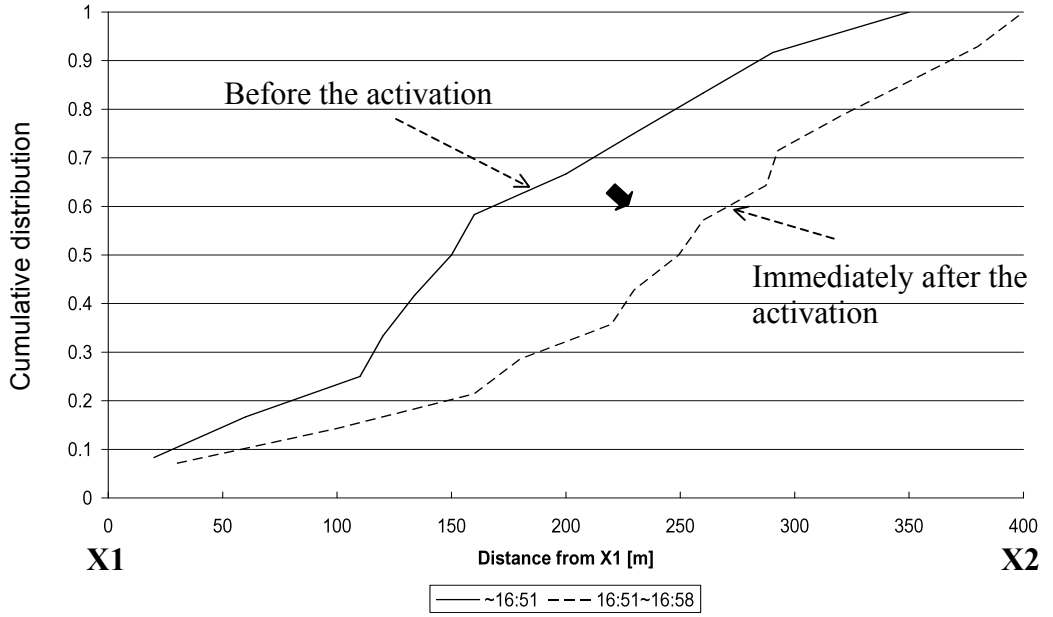

(b) Simulated

Figure 27. Comparison of cumulative distributions of R-F vehicles' lane changes from 5 to 4 before 16:58 hrs, SR-55N

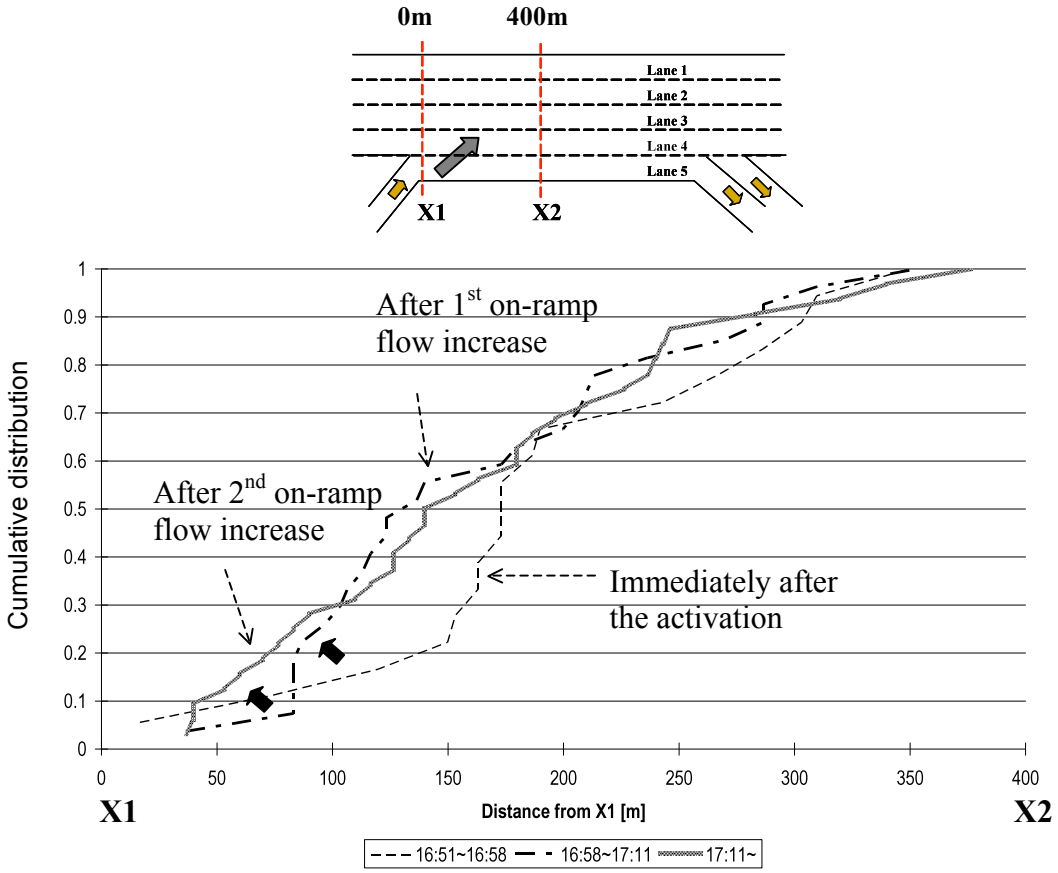

(a) Observed

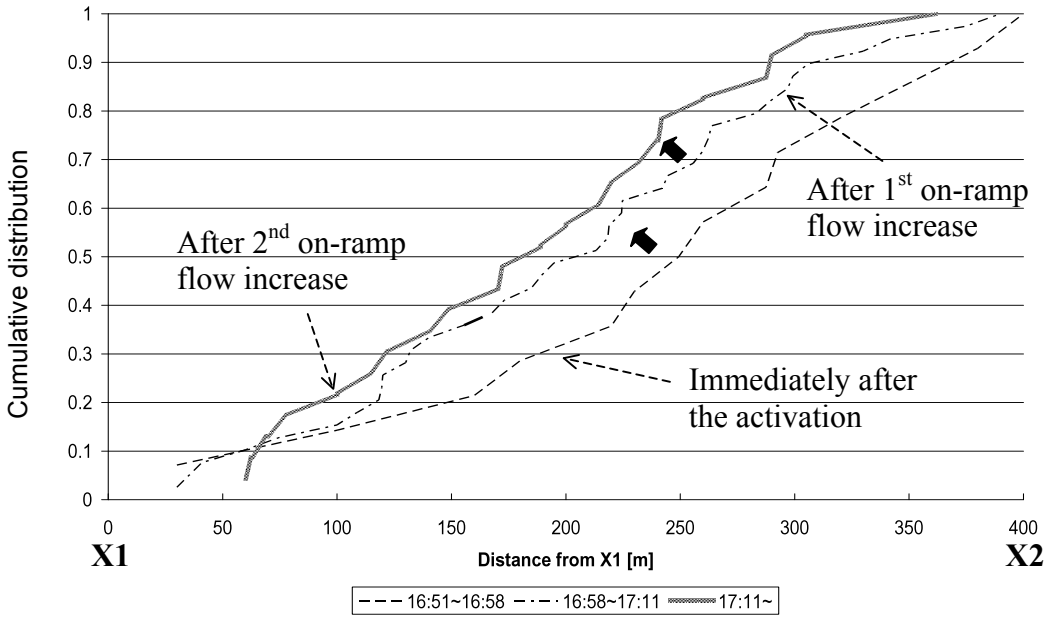

(b) Simulated

Figure 28. Comparison of cumulative distributions of R-F vehicles' lane changes from 5 to 4 after 16:51 hrs, SR-55N

4.3.2. Simulation Results for site 2, I-210 W

The model applied at site 1 (SR-55 N) was tested again at site 2 (I-210 W). Here the β estimated for site 1 were not altered in order to test the transferability of the estimated model; i.e., to investigate if this model can qualitatively replicate the traffic patterns at another site (site 2) without additional calibration. The input data for the simulations consisted of on-ramp demands (two R-R movements to account for the site's two off-ramps and one R-F movement, see again figure 15) and upstream freeway demands (one F-F and two F-R). Thus the site's two off-ramp junctions result in six distinct vehicular movements. Though the on-ramp was metered during the morning rush, on-ramp queues did not form during any of the observation periods. Hence, the measured on-ramp flows were equal to on-ramp demands. In contrast, queues formed in the upstream freeway segment during the rush periods, so freeway demands prior to the bottleneck activation were once again used for the whole simulated period, as previously explained in section 4.3.1.

Without the recalibration of the parameters, the model qualitatively replicated the O-curves and the cumulative distributions of lane changes observed at site 2. Figures 31a and b show the observed and simulated O-curves. The simulations accurately predicted the bottleneck activation time (6:54 hrs), the times when the discharge flows changed, and the directions of these changes. Figures 32a and b show the observed and simulated cumulative distributions of F-R vehicles' lane changes from 4 to 5, and figures 33a and b show these distributions for R-F maneuvers from 6 to 5. Figures 34 and 35 show these distributions for the period of demand fluctuation (reduction) from 6:57 to 6:59 hrs.

The simulated lane changes generally took place closer to the on-ramp than did their observed counterparts. These small discrepancies aside, the simulated maneuvers still qualitatively matched the observed ones fairly well: the cumulative distribution curves moved in the same directions from one time period to the next.

Further, the simulation results again showed that as F-R vehicles traveled on the upstream freeway segment and approached the merge, they postponed their maneuvers from lane 4 to 5 until reaching the location X1 where the auxiliary lane begins. Once these F-R vehicles passed the location X1 and encountered the auxiliary lane (with lower densities and higher speeds due to low on-ramp flows), they promptly maneuvered to lane 5, and then immediately onto lane 6, producing high concentrations of lane changes near the on-ramp.

In summary, the model qualitatively replicated observed lane-changing behavior and subsequent discharge flow changes at both weaving study sites.

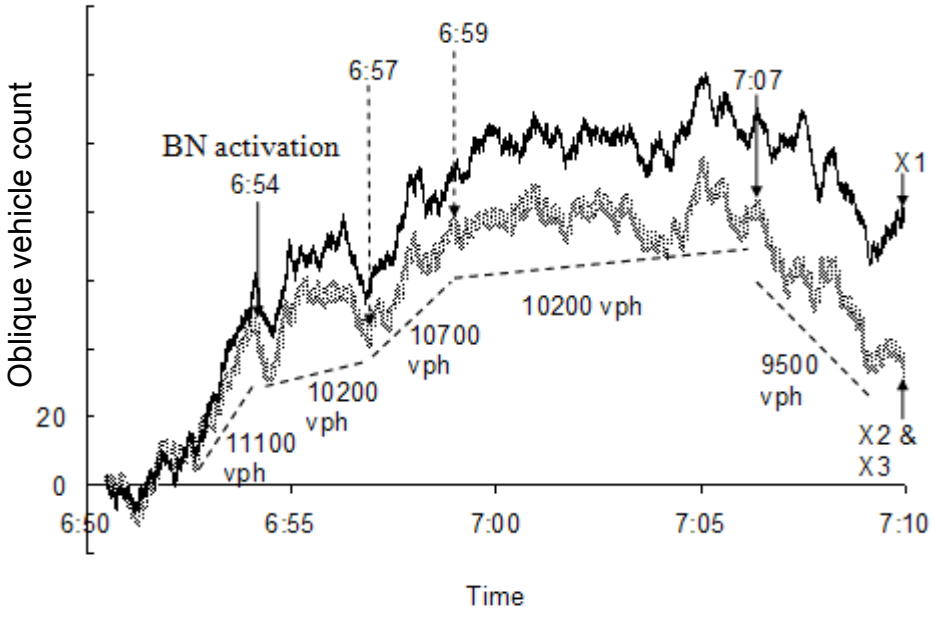

(a) Observed curves

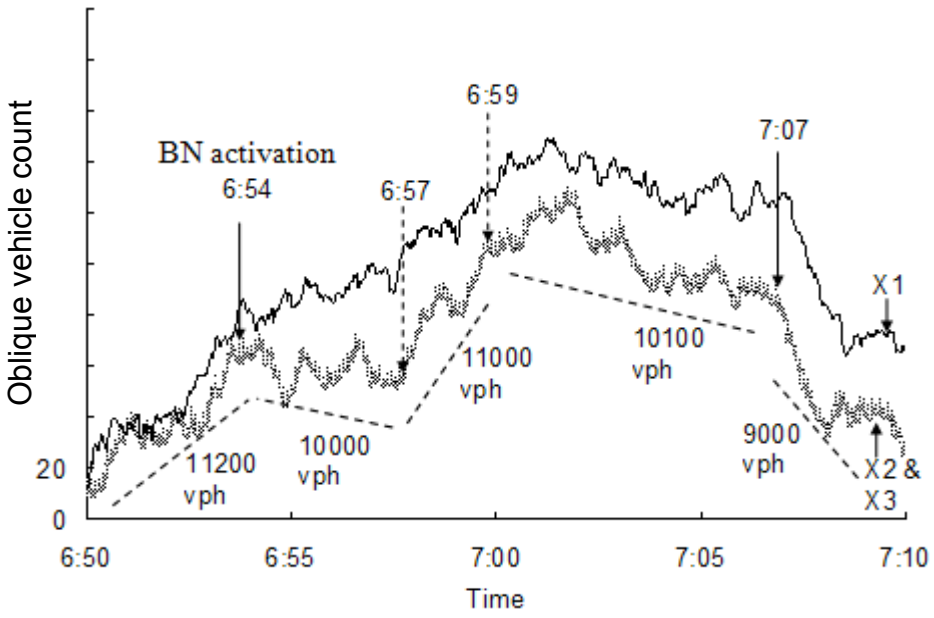

(b) Simulated curves

Figure 29. Comparison of oblique count curves at X1, X2, and X3, I-210 W

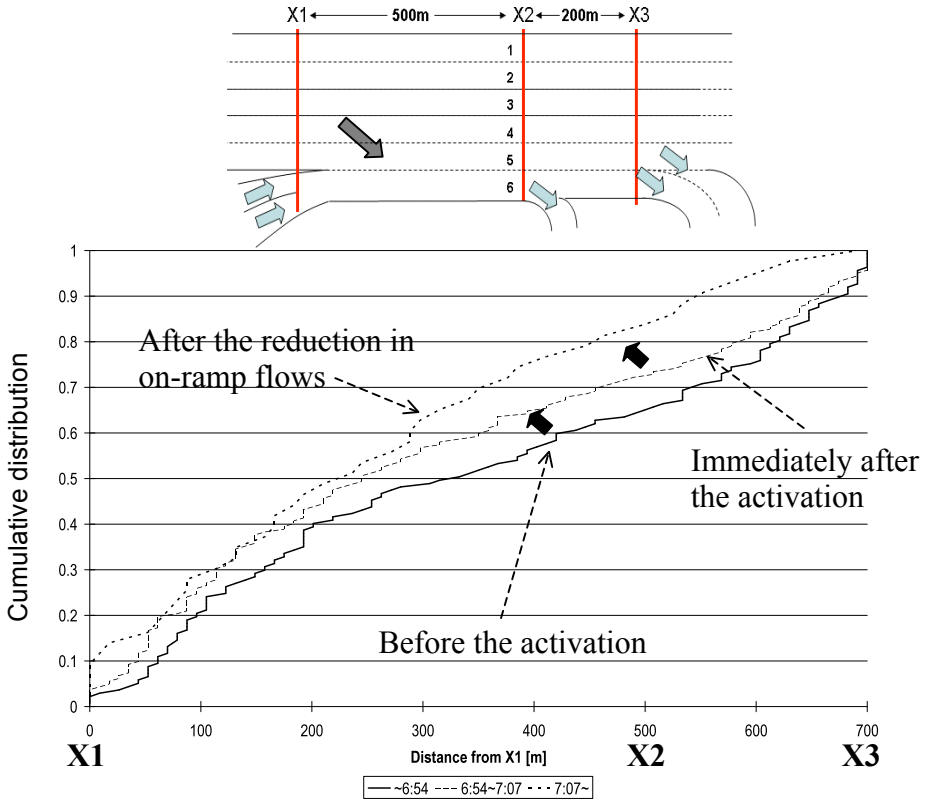

(a) Observed

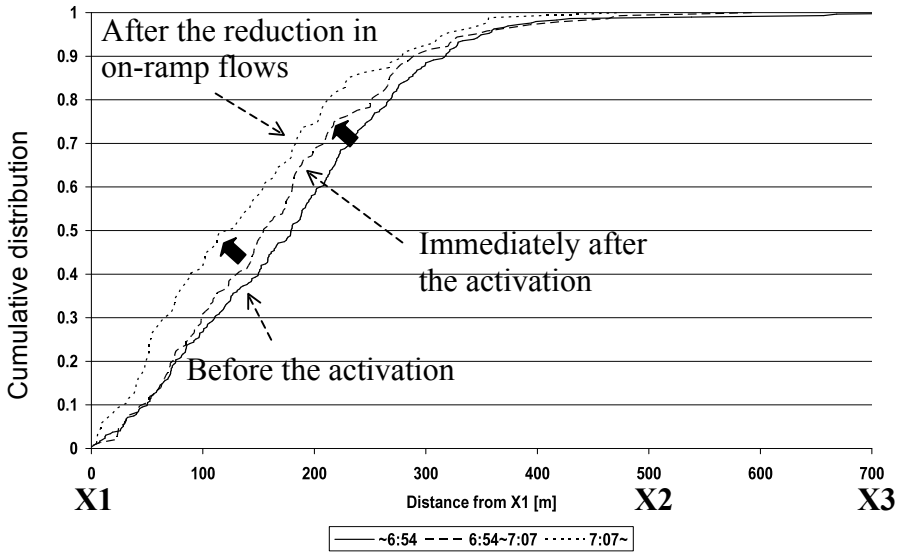

(b) Simulated

Figure 30. Comparison of cumulative distributions of F-R vehicles' lane changes from 4 to 5, I-210W

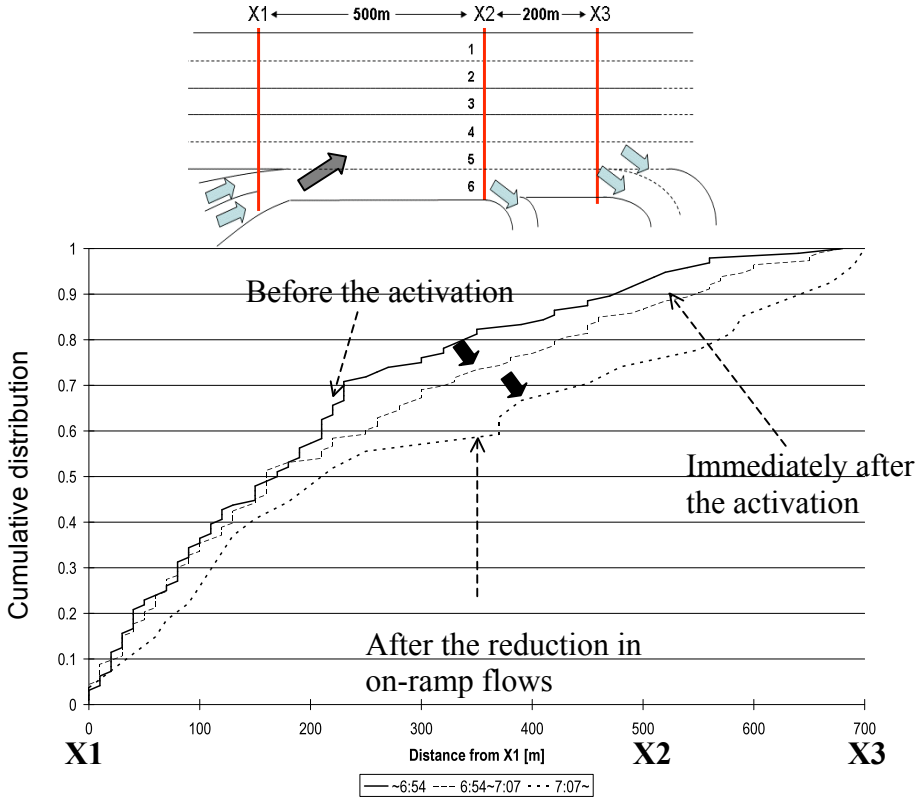

(a) Observed

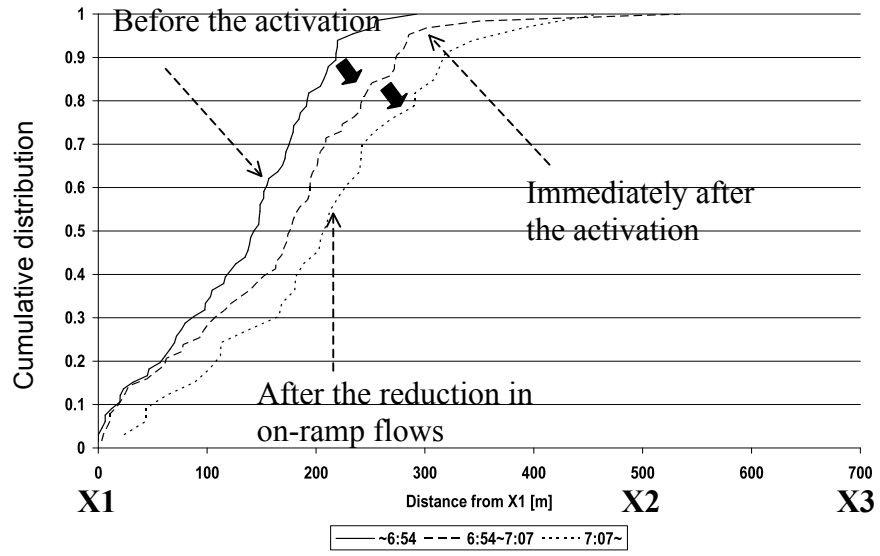

(b) Simulated

Figure 31. Comparison of cumulative distributions of R-F vehicles' lane changes from 6 to 5, I-210W

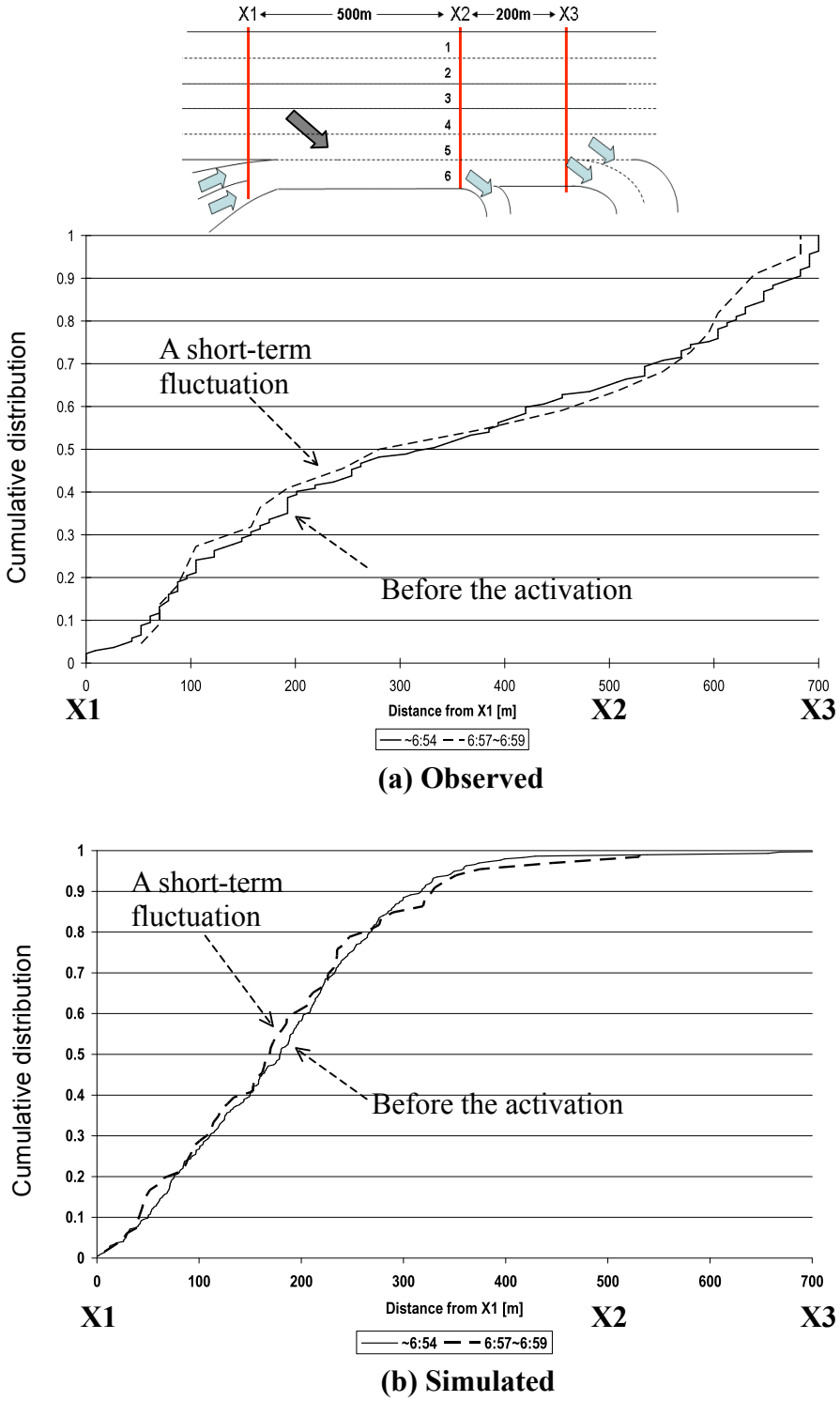

Figure 32. Comparison of cumulative distributions of F-R vehicles' lane changes from 4 to 5 between 6:57 hrs and 6:59 hrs, I-210W

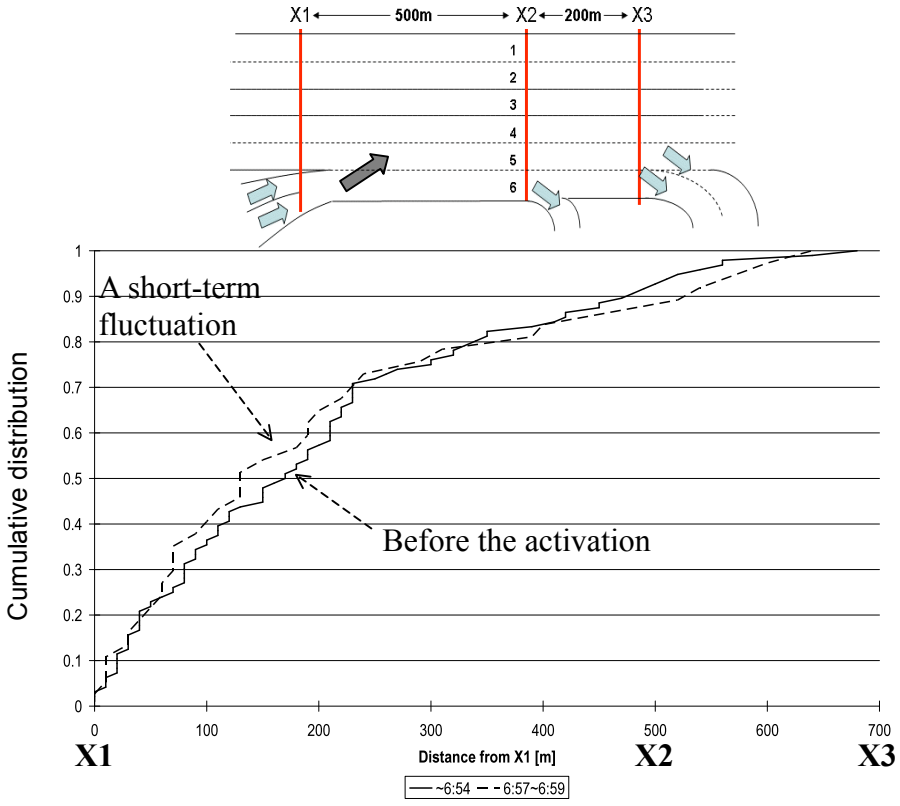

(a) Observed

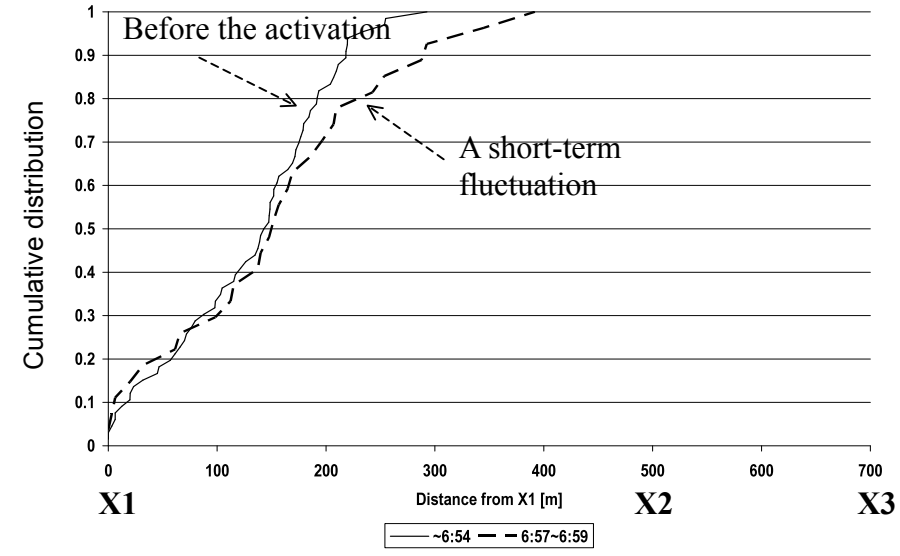

(b) Simulated

Figure 33. Comparison of cumulative distributions of R-F vehicles' lane changes from 6 to 5 between 6:57 hrs and 6:59 hrs, I-210W

CHAPTER 5. CONCLUSIONS

The investigations of the two weaving bottlenecks revealed that the bottleneck activations were triggered by disruptive F-R lane changes. F-R lane changes became disruptive: i) when there were increased concentrations of F-R lane changes near the on-ramp merge triggered by reductions in on-ramp flows; or ii) when there were simply too many F-R lane changes, independent of the ramp flows. The investigations further revealed that changes in the spatial distributions of mandatory lane changes, especially for the F-R maneuvers, also led to variations in bottleneck discharge flows. When the F-R maneuvers were concentrated near the on-ramp, they became more disruptive and resulted in discharge flow reductions. This cause and effect mechanism was verified from empirical findings in Chapter 3 and from the simulation results in Chapter 4.

Findings also indicate that the spatial distributions of these lane changes, in turn, were dictated by the traffic conditions in the auxiliary lane. On-ramp flow reductions evidently increased the attractiveness of the auxiliary lanes, thus motivating F-R drivers to perform their maneuvers nearer the on-ramp and to become more disruptive. In contrast, rising on-ramp flows reduced the attractiveness of the auxiliary lanes and reduced the amount of disruptive F-R maneuvers that took place near the on-ramp. These reductions led to discharge flow increases.

These mechanisms are contrary to the previous conjectures that higher on-ramp flows (more lane changes) decrease weaving bottleneck discharge flows. Yet, the data presented here are incontrovertible: it is not only the amount of lane changes that

influence weaving bottleneck discharge flows, but also the spatial distributions (the concentrations) of these maneuvers.

The observed phenomena also suggest that metering on-ramps at weaving sections can sometimes be detrimental to their discharge flows, possibly when the metering is very restrictive. Regretfully, the two sites reported here exhibited only a limited range of on-ramp flows. Thus, additional study sites may need to be analyzed to further our understanding of weaving bottlenecks, and to determine desirable ramp metering rates for these bottlenecks.

The model estimated in this work was based on observations of real traffic, and qualitatively reproduced the mechanisms of weaving bottleneck activations and discharge flow changes. The simulation results at both study sites supported the two key conjectures that arose from the empirical findings: i) traffic conditions (especially densities) in an auxiliary lane influence drivers' decisions on where to perform mandatory lane changes; and ii) the spatial distributions of these lane changes determine weave bottleneck discharge flows.

The model was developed into an executable standalone program in MATLAB so that engineers and planners can readily analyze and design freeway weaving sections. The user manual for this program is in Appendix B of this report. The program and its manual can be downloaded at the author's homepage (http://www2.decf.berkeley.edu /~ljunho7/weaving/).

REFERENCES

Ahmed, K. I. (1999), **Modeling drivers' acceleration changing behavior.** PhD thesis, Department of Civil and Environmental Engineering, Massachusetts Institute of Technology, MA, USA.

Ahn S. (2006), **Growth of oscillations in queued traffic.** PhD thesis, Department of Civil Engineering, University of California, Berkeley, CA, USA.

Bertini, R. L., Malik, S. (2004), **Observed dynamic traffic features on a freeway section with merges and divers**. *Transportation Research Record 1867,* pp. 25-35.

Cassidy, M. J. (2003), freeway on-ramp metering, delay savings and the diverge bottleneck**.** *Transportation Research Record 1856,* pp. 1-5.

Cassidy, M. J., Bertini R. (1999), **Some traffic features at freeway bottlenecks.** *Transportation Research Part B 33 (1)*, pp. 25-42.

Cassidy, M. J., Daganzo C. F. (2006), **Empirical Reassessment of Traffic Operations: Freeway Bottlenecks and the Case for HOV lanes.** *Report UCB-ITS-RR-2006-6*, Institute of Transportation Studies. University of California at Berkeley.

Cassidy, M. J., May, A.D. (1991), **Proposed Analytical Technique for Estimating Capacity and Level of Service of Major Freeway Weaving Sections.** *Transportation*

Research Record 1320, pp. 99-109.

Cassidy, M. J., Rudjanakanoknad, J. (2005), **Increasing the capacity of an isolated merge by metering its on-ramp.** *Transportation Research Part B 39 (1)*, pp. 896-913.

Cassidy, M., Skabardonis, A., May, A.D. (1989), **Operation of Major Freeway Weaving Sections: Recent Empirical Evidence.** *Transportation Research Record 1225*, pp. 61-72.

Cassidy, M. J., Windover, J.R. (1995), **Methodology for assessing the dynamics of freeway traffic flow.** *Transportation Research Record 1484*, pp. 73-79.

Daganzo, C.F. (2004), **In Traffic Flow, Cellular Automata = Kinematic Waves.** *Report UCB-ITS-RR-2004-5*, Institute of Transportation Studies. University of California at Berkeley.

Fazio, J., Rouphail, N. (1986), **Freeway Weaving Sections: Comparison and Refinement of Design and Operations Analysis Procedures.** *Transportation Research Record 1091*, pp. 101-109.

Fazio, J., Rouphail, N. (1990), **Conflict Simulation in INTRAS: Application to Weaving Area.** *Transportation Research Record 1287*, pp.96-107.

Glad, R. W., P.E., Milton, J. C., Olson, D. K. (2001), Weave **analysis and performance:**

the Washington state case study. *Research report WA-RD 515.1*, Washington state department of transportation, WA, USA.

Highway Capacity Manual (2000), **Weaving Segments.** Transportation Research Board, National Research Council, Washington D.C.

Windover, J. R., May, A. D. (1994), **Revisions to Level D Methodology of Analyzing Freeway Ramp Weaving Sections.** *Transportation Research Record 1457*.

Kwon, E. (1999), **Estimation of capacity in freeway weaving areas for traffic management and operations.** *Final report MN/RC-1999-40*, Minnesota department of transportation, MN, USA.

Kwon, E., Lau, R., Aswegan, J. (2000), **Maximum possible weaving volume for effective operations of ramp-weave areas.** *Transportation Research Record*, *1727*, Transportation Research Board, Washington, D.C., pp. 132–141.

Laval, J.A. (2004), **Hybrid models of traffic flow: impacts of bounded vehicle acceleration.** PhD thesis, Department of Civil Engineering, University of California, Berkeley, USA.

Laval, J. A., Daganzo, C.F. (2003**), A hybrid model of traffic flow: Impacts of roadway geometry on capacity.** TRB *2003 Annual Meeting CD-ROM.*

Laval, J. A., Daganzo, C.F. (2006), **Lane-changing in traffic streams.** *Transportation Research Part B 40(1)*, pp. 251-264.

Lertworawanich, P., Elefteriadou, L. (2002), **Capacity estimations for type-B weaving areas based on gap acceptance.** *Transportation Research Record 1776*, National Academy Press, pp. 24–34.

Lertworawanich P., Elefteriadou K. (2003), **A methodology for estimating capacity at ramp weaves based on gap acceptance and linear optimization.** *Transportation Research Part B 37,* pp. 459−483

Lertworawanich, P., Elefteriadou, L. (2004), **Evaluation of three freeway weaving capacity estimation methods and comparison to field data, freeway capacity.** *TRB Annual Meeting* _CD-ROM_,Washington, D.C.

Menendez, M. (2006), **An analysis of HOV lanes: Their impact on traffic.** PhD thesis, Department of Civil Engineering, University of California, Berkeley, USA.

Menendez, M., Daganzo, C. F. (2006), **Effect of HOV Lanes on Freeway Bottlenecks.** *Report UCB-ITS-VWP-2006-2*, UC Berkeley Center for Future Urban Transport: A VOLVO Center of Excellence. University of California at Berkeley.

Wang, M. H., Cassidy, M. J., Chan, P., May, A. D. (1993), **Evaluating the Capacity of Freeway Weaving Sections.** *Journal of Transportation Engineering, May/June 1993.*

Next Generation Simulation Community, **NGSIM**, http://ngsim.camsys.com/, 28 May 2005.

Pignataro, L., McShane, W., Roess, R., Crowley, K., Lee, B. (1975), **Weaving Areas-Design and Analysis.** *NCHRP Report 159*, pp. 119-120.

Rakha, H., Zhang, Y. (2004), **The INTEGRATION 2.30 framework for modeling lane-changing behavior in weaving sections.** *RB Annual Meeting* _CD-ROM_, Washington, D.C., paper # 04-3422.

Roess, R. (1987), **Development of Weaving Area Analysis Procedures for the 1985 Highway Capacity Manual.** *Transportation Research Record 1112*, pp. 17-22.

Roess, R., McShane, W., Pignataro, L. (1974), **Configuration and the Design and Analysis of Weaving Sections.** *Transportation Research Record 489*, Transportation Research Board, Washington, D.C.

Roess, RP, Ulerio JM (1999), **Weaving Area Analysis in the Year 2000 "Highway Capacity Analysis".** *Transportation Research Record 1710*, pp.145-153

Skabardonis, A., Cassidy, M., May, A.D., Cohen, S. (1989), **Application of Simulation to evaluate the Operation of Major Freeway Weaving Sections.** *Transportation Research Record 1225*, pp. 91-98.

Stewart, J., Baker, M., Van Aerde, M. (1996), **Evaluating weaving section designs using INTEGRATION.** *Transportation Research Record*, *1555*, Transportation Research Board, Washington, D.C., pp. 33–41.

Vermijis, R. (1998), **New Dutch capacity standards for freeway weaving sections based on micro simulation.** *Third Int. Symposium on Highway Capacity*, 1065-1080

Zarean, M., Nemeth, Z. A. (1988), **WEAVSIM: A microscopic simulation model of freeway weaving sections.** *Transportation Research Record 1194*, Transportation Research Board, Washington, D.C., 48-54

APPENDIX A: MENENDEZ'S CAR-FOLLOWING MODEL

The overview of Menendez's model was presented in section 2.4. Presented in this appendix is a more detailed qualitative description of the theory. The reader can refer to the original source – Menendez (2006) – to see the equations of the model. Section B.1 describes the car-following component of Menendez's model; and section B.2 explains the choice model for lane-changing.

A.1. Car-following Model

Menendez's model has three components in its car-following model: simple car-following, car-following during the lane-changing process, and cooperation and forced car-following for lane changes. The following sections explain the logic behind these three components.

A.1.1 Simple Car-following

The simple car-following model determines the locations of vehicles when there are no vehicles performing or attempting lane changes. Under this model, drivers maximize their traveled distance for each time interval subject to their vehicles' mechanical limitations, safety, and comfort.

The vehicles' mechanical limitations refer to the maximum acceleration and deceleration rates. Vehicles can only accelerate or decelerate based on these rates.

As regards to safety, the Menendez model does not allow any collisions during simulation runs. Rather, simulated vehicles must be able to slow down at any time without crashing into the vehicle in front. This safety constraint is based on equations developed from the time-space trajectories of two vehicles, assuming that the lead vehicle decelerates with the maximum rate and the reaction time of the following vehicle is one simulation interval.

Comfort constraints describe the relationship between a vehicle's spacing and its speed. This relationship is based on the CF(L) car-following model, something equivalent to the kinematic wave model, in which the vehicles' most advanced locations are the function of the difference between their current spacings and the jam spacing. Vehicles can *comfortably* travel at faster speeds as their spacings becomes larger.

A.1.2 Car-following during Lane-changing Process

The lane-changing model shares two constraints with the basic car-following model described above: mechanical limitations (i.e., vehicles can accelerate and decelerate with the maximum rates.) and safety. Regarding the later, vehicles that perform lane changes should not collide with any vehicles in the target lane. Note that this lane-changing model neglects the comfort constraint, because drivers tend to drive aggressively with lesser spacings when they change lanes.

A.1.3 Cooperation and Forced Car-following for Lane Changes

Safety constraints under simple car-following and lane changes become more restraining under congested traffic condition, resulting in the unrealistically small number of lane changes. To realistically replicate traffic behavior in congestion (to generate more lane changes), a logic of cooperation and forced car-following with lane changes is incorporated into the Menendez's model.

This logic is activated when a vehicle continuously tries and fails to perform a lane change based on the model in A.1.2. In this case, the lane-changing vehicle either slows down, or the vehicle behind in the target lane slows down to make space for her.

A.2. Choice Model for Lane-changing

The choice model determines when or where individual vehicles decide to perform lane changes. The choice model for lane-changing is composed of three components: mandatory time-related lane changes, mandatory space-related lane changes, and optional lane changes.

A.2.1 Mandatory Time-related Lane changes

The choice model describes a driver's lane-changing decisions in response to her perceptions of the HOV lane activation times. Single Occupancy Vehicle (SOV) drivers migrated from an HOV lane when they deem the HOV lane active, resulting in mandatory lane changes. The model randomly generates HOV activation times perceived

by individual drivers, and SOV drivers in the HOV lane perform lane changes according to these times.

A.2.2 Mandatory Space-related Lane changes

Vehicles perform mandatory space-related lane changes when there is a diverge or a lane-drop downstream. The decisions of where to perform these lane changes are determined by lane-changing cones (see figure 22). Note that this choice model is reworked in the present model, and for further explanations of this, see section 4.1.

A.2.3 Optional Lane changes

A driver's decision on optional lane changes is determined by the speed difference between her current lane and adjacent lanes, and her sensitivity to this difference; i.e., if a driver is sensitive, she reacts to slight differences in speeds.

APPENDIX B: THE MANUAL OF THE WEAVING SIMULATION PROGRAM

The following describes how to run the microscopic car-following and lane-changing simulation model of weaving traffic. Detailed algorithms for the simulation program were presented previously in this report. The program is only applicable to weaving sections with connected (full) auxiliary lanes. Applications of the program to acceleration or deceleration auxiliary lanes are not recommended. To download the zip file of the program, go to the following link: (http://www2.decf.berkeley.edu/~ljunho7/weaving/wsimv3.zip). First, extract the zip file onto your computer. If your computer does not have a zip program, go to this link to download one: (http://www.download.com/3001-2250_4-10631836.html). The program (a car-following with lane-changing model) simulates microscopic traffic behavior observed in freeway weaving sections.

To run this program, click the wsim.exe file and wait for a while (do not close the command prompt). If you receive any error messages while opening the program, go to the following link (http://www2. decf.berkeley.edu/~ljunho7/weaving/MCRInstaller.exe) and install the MCR installer program.

B.1. Inputs for the Program

Once the program is opened, users must specify several input items:

1) Traffic demands [veh/hr] by their Origin-Destination (i.e., Freeway-to-Freeway, Freeway-to-Ramp, Ramp-to-Freeway, and Ramp-to-Ramp) and the durations

[minutes] over which these rates persist. As many as 8 different OD tables can be run in a single simulation.

2) Geometric configurations:
    a. Length of the weaving section of interest [ft]
    b. Number of freeway lanes upstream of the on-ramp
    c. Number of off-ramp lanes
    d. Number of on-ramp lanes
    e. Free-flow speed for vehicles in simulation runs [mph]
    f. Reference speed for delay calculation [mph]

Two examples of geometric configurations are shown below in figure 38. Note that the program always assumes that there is at least one auxiliary lane from the on-ramp to the off-ramp.

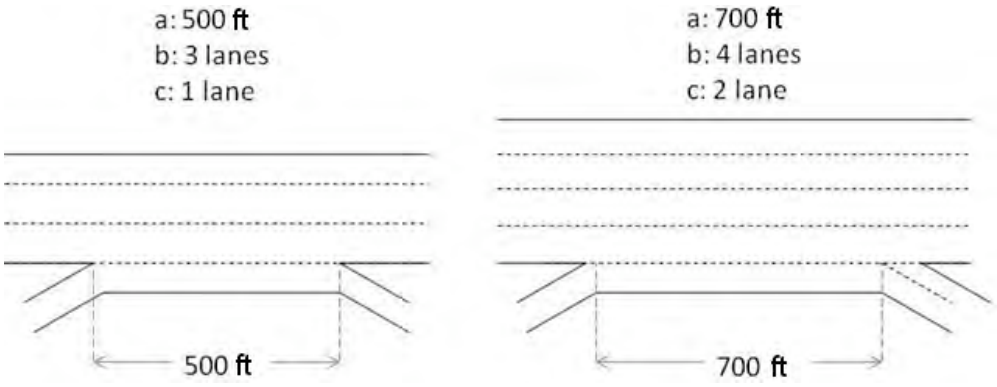

Figure 34. Examples of geometric configuration inputs for the program

B.2. Outputs of the Program

The program generates simulation results at one-minute intervals. It shows total delays [veh-hr] as well as delays [veh-hr] for each OD maneuver. Further, it plots oblique cumulative vehicle count curves (O-curves) that display freeway and off-ramp discharge flows [veh/hr]. It also displays time-series of one-minute average speeds by OD maneuvers:

1) Solid line in red: average speeds of F-F traffic
2) Solid line in green: average speeds of F-R traffic
3) Dotted line in blue: average speeds of R-F traffic
4) Dotted line in black: average speeds of R-R traffic

B.3. Program Reports

The report button on the main menu generates report of simulation results on two different windows. The first window displays:

1) Demands specified by the user
2) Geometric configurations of the weaving section
3) Total delays and delays by OD
4) Average freeway and off-ramp discharge flows
5) The O-curve of freeway flows of the weaving sections' downstream end
6) The O-curve of off-ramp flows
7) The time-series curve of the weaving section's total density
8) The time-series curves of vehicular speed by OD

The second window displays the following information for each user-specified period:

1) The O-curve of freeway flows of the weaving sections' downstream end & off-ramp flows
2) Average speeds of all vehicles and vehicular delays
3) The average speeds and delays for each OD maneuver

The report is automatically saved as a report.bmp file and a report_by_period.bmp file at the location where the program is installed. Users can easily import these image files into any software applications. Sometimes one of the report windows is not saved in the image files due to some unknown bugs in Matlab. If this happens, click the report button again without closing any windows.